ORNL/Sub-81/21086/2
WFPS:TME-81-026
July 1, 1981
UC-20a

FINAL REPORT
PHASE II - EBT-S DIVERTOR PROJECT

ENGINEERING DESIGN OF A TOROIDAL DIVERTOR FOR THE EBT-S FUSION DEVICE

Principal Investigator Phase I, L. P. Mai
Principal Investigator Phase II, F. S. Malick
Project Manager, G. Gibson

Prepared for

Oak Ridge National Laboratory
Oak Ridge, Tennessee 37830
Operated by
Union Carbide Corporation
for the
U.S. Department of Energy
Contract No. W-7405-eng-26

Prepared by

Westinghouse Electric Corporation
Fusion Programs Department
P. O. Box 10864
Pittsburgh, Pennsylvania 15236-0864
Under Subcontract No. 22X-21086C

ACKNOWLEDGEMENTS

This work was performed for the Union Carbide Corporation Nuclear Division under Subcontract No. 22X-21086C. Reproduction, translation, publication, use and disposal, in whole or in part, by or for the United States Government is permitted.

In order to complete this study successfully a great deal of interaction was required with ORNL personnel regarding the EBT-S device and facility. We wish to thank R. Colchin for his guidance, L. Berry and J. Sheffield for their support, and G. Hastie, R. Livesey, D. Everet, and T. Tucker for their reviews, comments, and recommendations. These scientists and engineers are all with the Oak Ridge National Laboratory.

The typing and assembly of the report was the responsibility of Yvonne Harlow.

Printed in the United States of America
Available from
National Technical Information Service
U.S. Department of Commerce
5285 Port Royal Road
Springfield VA 22161

NTIS Price Codes
Printed Copy: A05
Microfiche: A01

ORNL/Sub-81/21086/2
WFPS:TME-81-026
July 1, 1981
UC-20a

FINAL REPORT
PHASE II - EBT-S DIVERTOR PROJECT

ENGINEERING DESIGN OF A TOROIDAL DIVERTOR FOR THE EBT-S FUSION DEVICE

CONTRIBUTORS:

W. C. Brenner, R. Chianese, G. Gibson, F. M. Heck, E. M. Iwinski,
A. Y. Lee, F. S. Malick, D. A. Sink, R. W. Stooksberry

APPROVED BY: ______________________

G. Gibson,
Project Manager

APPROVED BY: ______________________

T. C. Varljen, Manager
Engineering

Westinghouse Electric Corporation
Fusion Programs Department
P. O. Box 10864
Pittsburgh, PA 15236-0864

ABSTRACT

The mechanical, structural, thermal, electrical, and vacuum design of a magnetic toroidal divertor system for the Elmo Bumpy Torus (EBT-S) is presented. The EBT-S is a toroidal magnetic fusion device located at the ORNL that operates under steady state conditions. The engineering of the divertor was performed during the second of three phases of a program aimed at the selection, design, fabrication, and installation of a magnetic divertor for EBT-S. The magnetic analysis of the toroidal divertor was performed during Phase I of the program and has been reported in a separate document. In addition to the details of the divertor design, the modest modifications that are required to the EBT-S device and facility to accommodate the divertor system are presented.

TABLE OF CONTENTS

Section . . . Page

1.0 INTRODUCTION . . . 1-1

1.1 Features of the Toroidal Divertor System . . . 1-2

2.0 DESCRIPTION OF THE EBT-S TOROIDAL DIVERTOR DESIGN . . . 2-1

2.1 Divertor Integration into EBT-S . . . 2-1
2.2 Divertor General Arrangement . . . 2-6
2.3 Design of Divertor Coils . . . 2-9
2.3.1 Coil No. 1 . . . 2-12
2.3.2 Coil No. 2 . . . 2-15
2.3.3 Coil No. 3 . . . 2-15
2.3.4 Coil No. 4 . . . 2-18
2.3.5 Electrical Circuit for the Divertor Coils . . . 2-20
2.3.6 Water Cooling of the Divertor Coils . . . 2-21
2.3.7 X-Ray Dose to Coil Insulation . . . 2-24
2.3.8 Summary of Forces and Torques . . . 2-27
2.4 Divertor Coil Enclosure . . . 2-29
2.5 Removable Targets . . . 2-33
2.5.1 Erosion of the Targets . . . 2-33
2.6 Divertor Cavity . . . 2-37
2.7 Mirror Coils . . . 2-39
2.8 Vacuum Pumping of the Divertor Chambers . . . 2-41
2.8.1 Microwave Shielding . . . 2-46
2.9 Diagnostic Instrumentation . . . 2-47

3.0 MODIFICATIONS TO THE EBT-S DEVICE AND FACILITY . . . 3-1

3.1 Device Modifications Which Are Part of the Divertor Assembly . . . 3-1
3.2 Device Modifications Which Are Not Part of the Divertor Assembly . . . 3-1
3.3 Facility Additions . . . 3-3
3.4 Additional Divertor Assembly Components . . . 3-4

4.0 CONCLUSION . . . 4-1

5.0 REFERENCES . . . 5-1

APPENDIX I: SYSTEMATIC METHOD OF ADJUSTING THE DIVERTOR MAGNETIC FIELD CONFIGURATION . . . I-1

LIST OF FIGURES

Figure No.	Title	Page
1-1	Schematic Layout of EBT-I/S	1-4
1-2	Three-Dimensional Pictorial Display of Toroidal Divertor and Two Adjacent Mirror Coils; Oblique View	1-5
1-3	Horizontal Cross Section Through the Toroidal Divertor Assembly with Diverted Flux Lines Superimposed	1-6
2-1	Plan View which Shows how the Divertor Cavity, with its Two Adjacent Mirror Coils, can be moved into the Opening in the Torus	2-2
2-2	Plan View of Divertor with Pumping Panels Showing Interfaces with the Existing EBT-S	2-4
2-3	Elevation View of Divertor on Section A-A of Figure 2-2 Showing the Interfaces with the Existing EBT-S	2-5
2-4	Horizontal Cross Section Through the Toroidal Divertor Assembly	2-7
2-5	Options for Conductor Turn-to-Turn Transitions in Coils	2-13
2-6	Coil and Lead Configuration of Coil #1, the Main Divertor Coil	2-14
2-7	Coil and Lead Configuration of Coil #2, one of the Main Divertor Pancake Coils	2-16
2-8	Conductor and Lead Configuration for Coil #3, the Outermost Divertor Coil	2-17
2-9	Coil and Lead Configuration of Coil #4, a Divertor Compensating Coil	2-19
2-10	Schematic Representation of the Proposed Divertor Coil Excitation Approach	2-22
2-11	Divertor Coil Enclosure Tube Patterns Showing that the Removable Target Overlaps the Coil Enclosure and Showing Water Headers which Provide for Water Flow in Opposite Directions in Adjacent Tubes	2-31
2-12	Elevation View of the Tube Pattern for the Removable Targets Showing the Wider Tube Spacing at the Corners	2-34
2-13	Elevation View of the Side of the Divertor Cavity Showing the Notch in the Cover Plate which Provides Clearance for the Mirror Coil Bus Bars	2-38

LIST OF FIGURES (Continued)

Figure No.	Title	Page
2-14	Horizontal Plane Cross Section Through the Divertor Cavity Showing the Components of the Weldment Assembly and the Machining-Centers and Axes	2-40
2-15	Plan View of the Divertor with Pumping Panels Showing Interfaces with the Existing EBT-S	2-42
2-16	Elevation View of the Divertor on Section A-A of Figure 2-2 Showing the Interfaces with the Existing EBT-S	2-43
2-17	Cross Section and Elevation View of the Cryopanels in the 90° and 270° Sectors of the Divertor Cavity	2-45
2-18	Sketch of Expected Power Density Profile (Inner Target Collector	2-49
2-19	Tentative Thermocouple Location Map for Removable Inner Target Collector	2-50
2-20	Thermocouple Mounting Detail Drawing	2-51
2-21	Field-of-View for the Infrared Camera Diagnostic; Plan View	2-54
2-22	Field-of-View for the Infrared Camera Diagnostic; Elevation View	2-55

LIST OF TABLES

Table No.	Title	Page
1-1	Conclusions and Recommendations Based on Phase I Results	1-2
1-2	Summary of Parameters for the EBT-S Toroidal Divertor	1-8
2-1	Divertor Coil Current, Loss, and Water Cooling Data	2-23
2-2	Summary of Parameters for the EBT-S Divertor Water Cooling System	2-32
3-1	Divertor Components Which Are Not Device Modifications	3-4

1.0 INTRODUCTION

Westinghouse Fusion Power Systems Department, under contract to the Oak Ridge National Laboratory (ORNL), has completed Phase II of a two-phase program to design a divertor system for the EBT-S[1-2] device which is located at the ORNL Y-12 site. The engineering design of a divertor that resulted from the Phase II program is presented in this report. Phase I of this study was completed in January of 1981, and the results of that study were published in reference 3. A summary of the conclusions and recommendations from the Phase I study are shown in Table 1-1. These recommendations were approved by the ORNL and formed the basis for the Phase II study.

Although it was shown during Phase I that it would be feasible to add either a toroidal or a bundle divertor to EBT-S, a toroidal divertor which is centered about a vertical plane located midway between adjacent mirror coils was chosen as the divertor to be engineered. The remainder of the recommendations in Table 1-1 have also been incorporated into the divertor design. During Phase I, sufficient engineering of the divertor systems was performed to demonstrate feasibility. Although the magnetic designs, i.e., the number, location, and ampere-turns of the coils, have not been altered during Phase II, many mechanical and thermal design changes have resulted. In fact, for some of the components, such as the divertor coils, several different designs were engineered and analyzed. However, in this report the emphasis is on the final design that evolved as the work progressed. In general, the intermediate designs will not be discussed to avoid any confusion with the design as it existed at the end of Phase II. The modifications that are required to the EBT-S device and facility to accommodate the divertor system have been kept to a minimum. These modifications are also described in this report.

Based on the design developed during Phase II, a program plan and budgetary cost estimate have been obtained for Phase III. Phase III includes the final design, fabrication and procurement of components, assembly, and installation of the divertor into EBT-S. The program plan and cost estimate for Phase III

TABLE 1-1

CONCLUSIONS AND RECOMMENDATIONS BASED ON PHASE I RESULTS

CONCLUSION

It Is Feasible To Add Either A Toroidal Or A Bundle Divertor To EBT-S In Order To Experimentally Study The Impact On The Plasma Performance And Stability.

RECOMMENDATIONS

1) Toroidal Divertor Centered Midway Between Adjacent Mirror Coils

2) Neutralizing Target

3) Initial Pumping System

- Two Turbomolecular Pumps; 2400 ℓ/s for H_2 [Based On Low Pumping Speed/High Recycle (82%)]

- Poloidal Compartments In Divertor Chamber; Walls Located At ± 30° About Equatorial Plane On Inside Portion Of Torus

- Test Of ZrAl Getter Panel Section

4) Design Divertor Chamber So That ≈ 1.4 m^2 Of Pumping Panel Can Be Added as an Upgrade In Order That High Pumping Speed/Low Recycle Mode Of Operation Can Be Tested

---

are presented in a separate report issued to the ORNL. Phase III remains to be authorized, pending a review of the Phase II design and cost estimates.

1.1 FEATURES OF THE TOROIDAL DIVERTOR SYSTEM

The toroidal divertor concept has been analyzed and described in depth in Reference 3. However, for completeness, some of the features of the divertor system are presented here in the introduction prior to launching into the engineering sections.

Figure 1-1 is a trimetric layout of the EBT-S device. The toroidal divertor would be installed in one of the twenty-four cells of the torus. Figure 1-2 is a three-dimensional pictorial display of the toroidal divertor coils relative to the two adjacent mirror coils. The currents in the main divertor coils flow in the opposite direction to the currents in the mirror coils. This is essential in order to create a separatrix and field null. The sum of the ampere-turns required in the main divertor coils is 62% of the ampere-turns in a mirror coil for the reference operation. The currents in the compensating coils flow in the same direction as the currents in the mirror coils and the ampere-turns per compensating coil is one-half of the total ampere-turns in the main divertor coils. Thus, the divertor coil system adds no net ampere-turns to the torus. The coils and power supply system are designed so that the current in the divertor coils can be changed by ± 20%. This will result in changing the location of the separatrix, and therefore the scrape-off layer thickness, by ± 1 cm. Figure 1-3 shows a cross section in the horizontal symmetry plane of the divertor cell. The scrape-off layer for the reference operating conditions is superimposed on the drawing.

It can be seen in Figure 1-3 that the divertor coils are located external to the torus vacuum system and that the water-cooled enclosure for the main divertor coils creates two divertor chambers. There is a plasma neutralizing target in each chamber capable of dissipating 200 kW of power. The targets are water-cooled copper, clad with tungsten to inhibit sputtering. However, TiC clad targets may also be tested during the experimental program. These targets extend ± 45° about the equatorial plane on the inner side of the torus. Because of the nature of the charged-particle drift surfaces most of the charged particles escaping from the torus should impinge on these targets. The targets have been designed for easy replacement.

Coils have been designed that fit in the available space, have adequate cooling, and their leads introduce little field error. Furthermore, the coils have been designed so that they can be powered by one of the existing motor-generator sets at the Y-12 site.

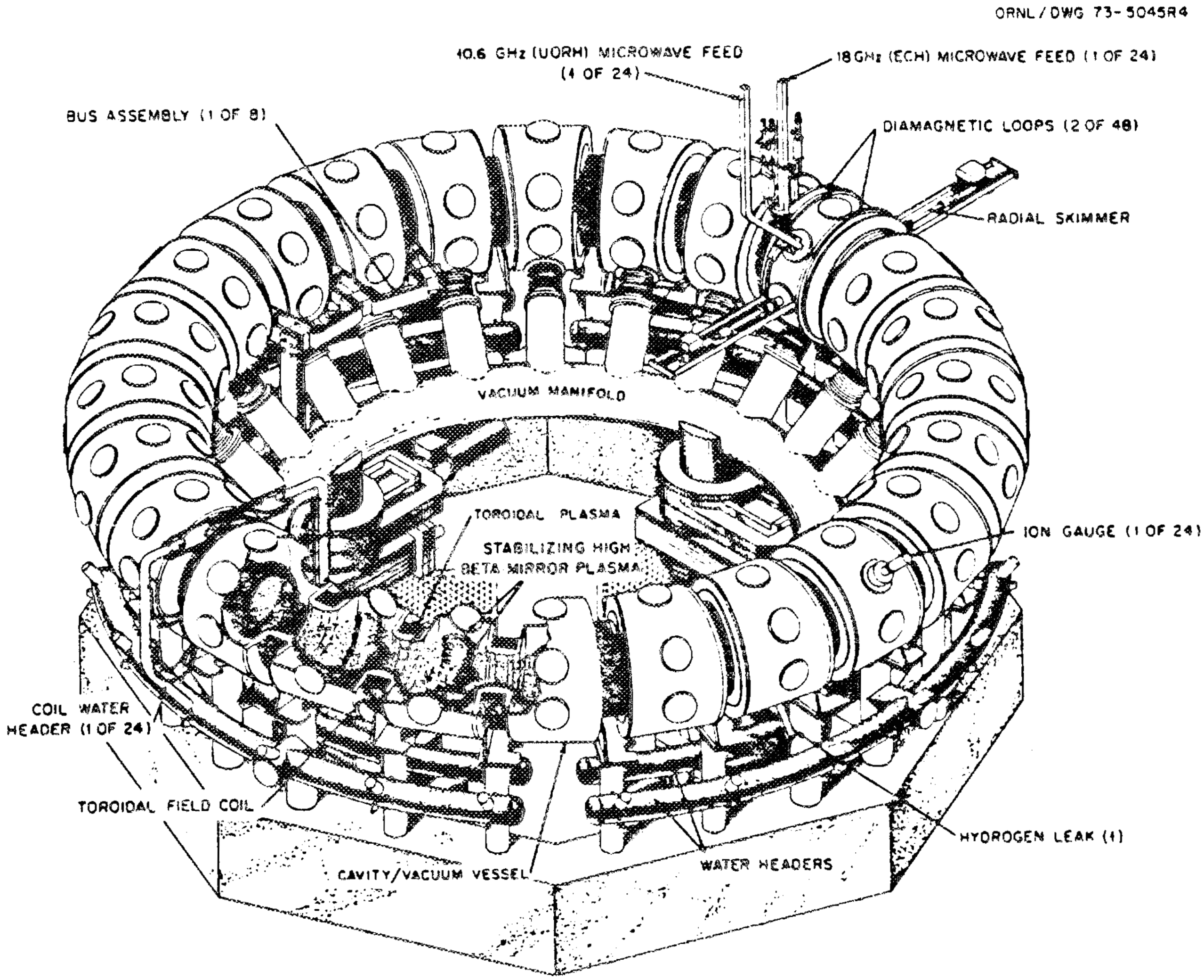

Figure 1-1. Schematic Layout of EBT-I/S

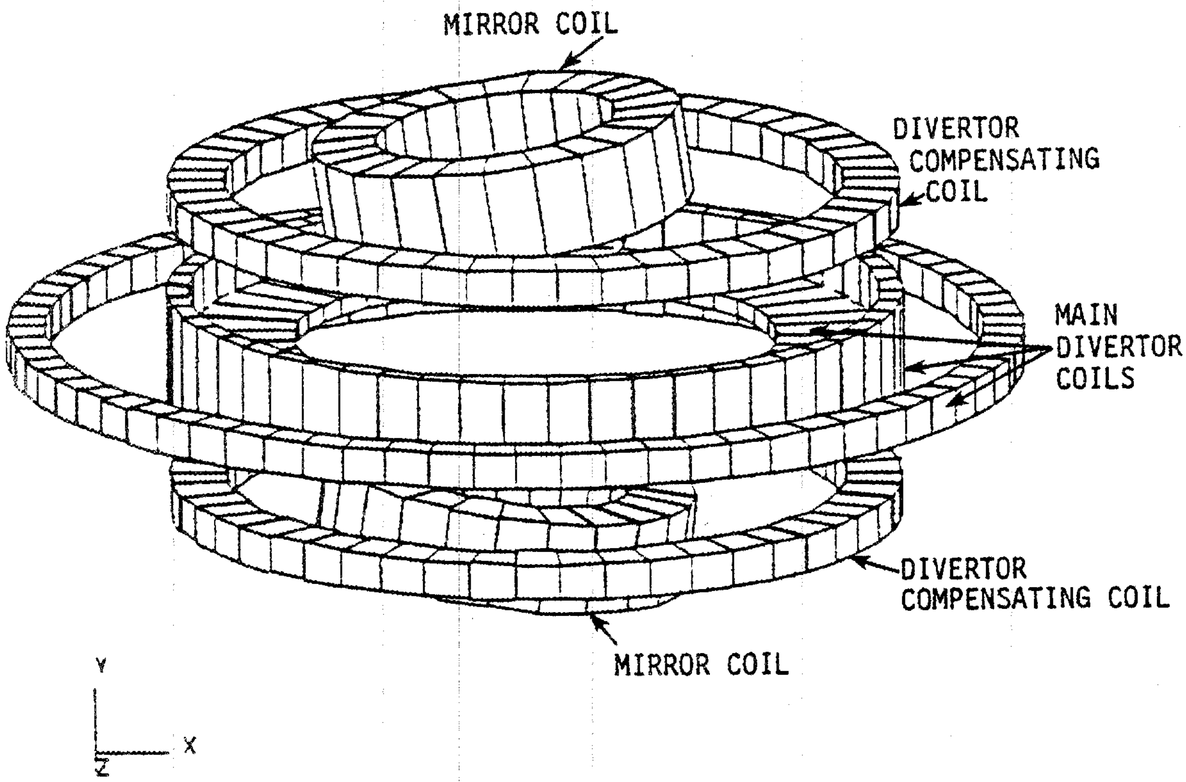

Figure 1-2. Three-Dimensional Pictorial Display of Toroidal Divertor and Two Adjacent Mirror Coils; Oblique View

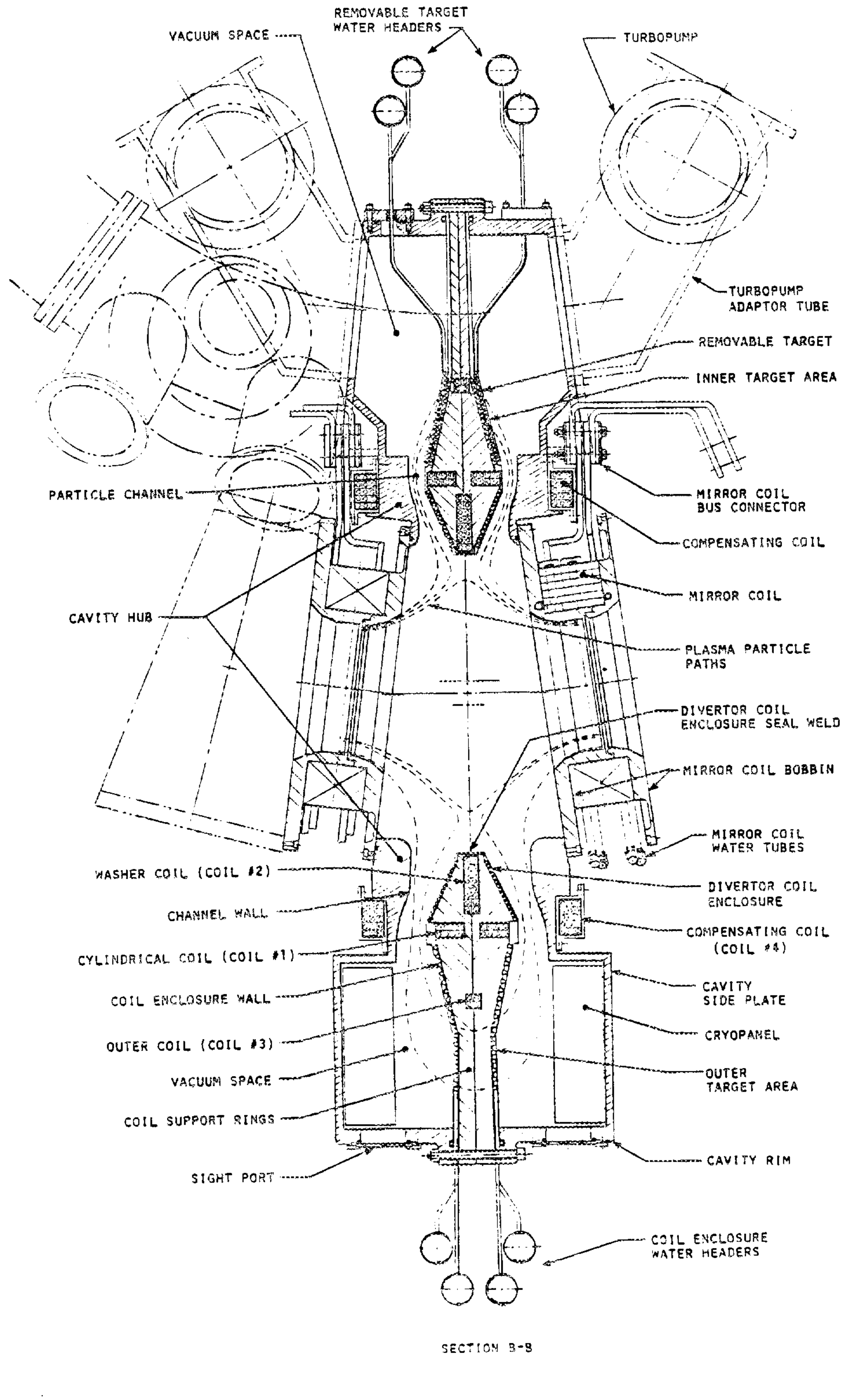

Figure 1-3. Horizontal Cross Section Through the Toroidal Divertor Assembly with Diverted Flux Lines Superimposed

Initially the divertor will operate in the high recycle/low pumping speed mode. Pumping will be provided by two turbomolecular pumps, one on each of the two divertor chambers. As described in reference 3, each chamber is divided into two compartments in the poloidal direction to enhance the vacuum pumping. However, the divertor chamber has been designed so that 1.4 m^2 of pumping panel can be introduced as a later upgrade to the system. With these pumping panels installed, the system will operate in the low recycle/high pumping speed mode. To aid in the selection of the pumping panels, i.e., ZrAl getter panels vs cryopanels, a section of a ZrAl panel will be installed and tested during the initial experimental phase.

A summary of the divertor characteristics and parameters are presented in Table 1-2. The development of these parameters is discussed in Sections 2.0 through 2.8.

The divertor cell including the two adjacent mirror coils, as shown in Figure 1-3, will be assembled and installed as a unit into the EBT-S device. Rather modest modifications are required to the EBT-S device and facility. These modifications are discussed in Section 3.0.

TABLE 1-2

SUMMARY OF PARAMETERS FOR THE EBT-S TOROIDAL DIVERTOR

General Parameters

Divertor Occupies One Cell of the EBT-S	
Number of Divertor Coils	5
Number of Main Divertor Coils	3
Number of Compensating Divertor Coils	2
Shape of Coils	Circular
Dimensions of Copper Conductor for All Coils	1.17 cm x 1.17 cm
Diameter of Conductor Water Coolant Channel	0.65 cm
Weight of Divertor Assembly (with Mirror Coils)	2500 lb

Coil Dimensions

Coil ID	Number of Coils (#)	Major Radius (cm)	Minor Radius (cm)	Axial Displacement (cm)	Axial Dimension (cm)	Radial Dimension (cm)
Mirror	24	150	16.39	-	10.2	6.94
1	1	152	38	0	12.0	2.4
2	1	152	31.3	0	2.0	11.0
3	1	150	52	0	4.0	4.0
4	2	152	36	± 16.5	4.0	6.0

Electrical Characteristics

Coil Identification Number	1	2	3	4
Total Turns	16	16	4	15/Coil
Current*/Conductor (A)	7893	3750	3000	6600
Connection Type	Series	Parallel†	Parallel†	Series
Terminal Current (A)	7893	7500	6000	6600
Ampere-Turns	126,300	60,000	12,000	99,000/Coil
Coil Voltage (V)	64.5	12.4	4.3	91.8
Power Loss/Coil (kW)	509	93.3	25.8	605

All Coils Are Connected in Series (with shunts) and Powered by a 3 MW Generator Rated at 350 V that Exists at the ORNL Y-12 Site.

---

*For fine tuning and experimental flexibility the currents can be varied ± 20%.
†Two conductors in parallel acting as one electrically, but providing two water circuits.

TABLE 1-2 (CONTINUED)

Coil Water-Cooling Parameters

Coil Identification Number	1	2	3	4
Number of Water Circuits	16	4	2	30
Loss Per Water Circuit* (kW)	36.6	23.3	12.9	21.3
Circuit Flow Rate (kg/s)	0.190	0.096	0.053	0.112
Coil Flow Rate (kg/s)	3.05	0.384	0.106	3.36
Maximum Flow Velocity (m/s)	5.78	2.91	1.61	3.40
Circuit Pressure Drop (kPa)	446	289	27.7	126

Target Water-Cooling Parameters

Particles Deposit on Water-Cooled Copper Surfaces
Copper is Clad with W or TiC to Prevent Sputtering
Maximum Power Deposited on Each Divertor Target - 200 kW

Divertor Water-Cooling Parameters

	Removable Target	Coil Enclosure: Inner Ring	Outer Ring
No. of Tubes	20	13	17
Avg. Length of Tube, cm	156	295	378
Longest Length of Tube, cm	181	315	410
Heated Length of Tube, cm	165	307	308
Design Power Density, kW/cm	0.22	0.15	0.15
Water Velocity, m/s	5.95	7.39	10.36
Water Flow Rate, kg/s (gpm)	2.36(39)	1.94(32)	3.55(58)
P, MPa (psi)	0.17(24.5)	0.39(56.7)	0.89(129.6)

Divertor Vacuum System

H-Atom Flow to Divertor Chambers (s^{-1})	1×10^{20}
Hydrogen Flow to Divertor Chambers (torr-ℓ s^{-1})	1.5
Microwave Shielding Provided for Pumping Systems	
Low Pumping Speed/High Recycle, 82%:	
Pumping Speed for Each of Two Turbo Molecular Pumps (ℓs^{-1}, H_2)	1150
Maximum Pressure in Divertor Chamber (torr)	1.4×10^{-4}
High Pumping Speed/Low Recycle, 10% (Requires Upgrade):	
Pumping Panels; Either Cryopanels or ZrAl Getter Panels	
Pumping Panel Area (m^2)	1.4
Pumping Speed (ℓ cm^{-2} s^{-1}, H_2)	10
Maximum Pressure in Divertor Chamber (torr)	2.3×10^{-5}

*Including leads

2.0 DESCRIPTION OF THE EBT-S TOROIDAL DIVERTOR DESIGN

The objective of this section is to present a complete picture of the design of the divertor as it existed at the end of Phase II. The magnetic analysis work which led to the coil design is adequately presented in the Phase I report (Reference 3). Analyses which support the design are also presented in this section.

2.1 DIVERTOR INTEGRATION INTO EBT-S

The size of the toroidal divertor relative to the EBT-S device can be readily appreciated from Figure 2-1 which shows the EBT-S with the divertor inside the walls which provide radiation shielding. The diameter of the divertor was limited by the constraint that no notch be cut into the concrete curb supporting the EBT-S torus.

The divertor is designed to be assembled with its two adjacent mirror coils and moved as a unit on a special transport dolly into the radiation shield room. It is then positioned in a gap in the torus as shown in Figure 2-1. A special transport dolly is required because the final movement of the divertor into the gap must be horizontal. Since the curb will prevent the dolly from being wheeled into the torus, riggers will slide the divertor assembly into position along the surface of the dolly. There is insufficient space above the cavity for an overhead crane. Furthermore, access is limited above the device by the cable tray and diagnostic components.

In Figure 2-1 the divertor is shown in cavity location W-2, but the design of the divertor would be the same for any of the four locations designated with the number 2. The final location selection has not been made but locations W-2 and N-2 are favored because they are close to the entrance and will cause less disturbance to the installed diagnostics during installation and any repair activities. Furthermore, background noise from the divertor chambers will be less likely to perturb any detector signals. The number 2 locations

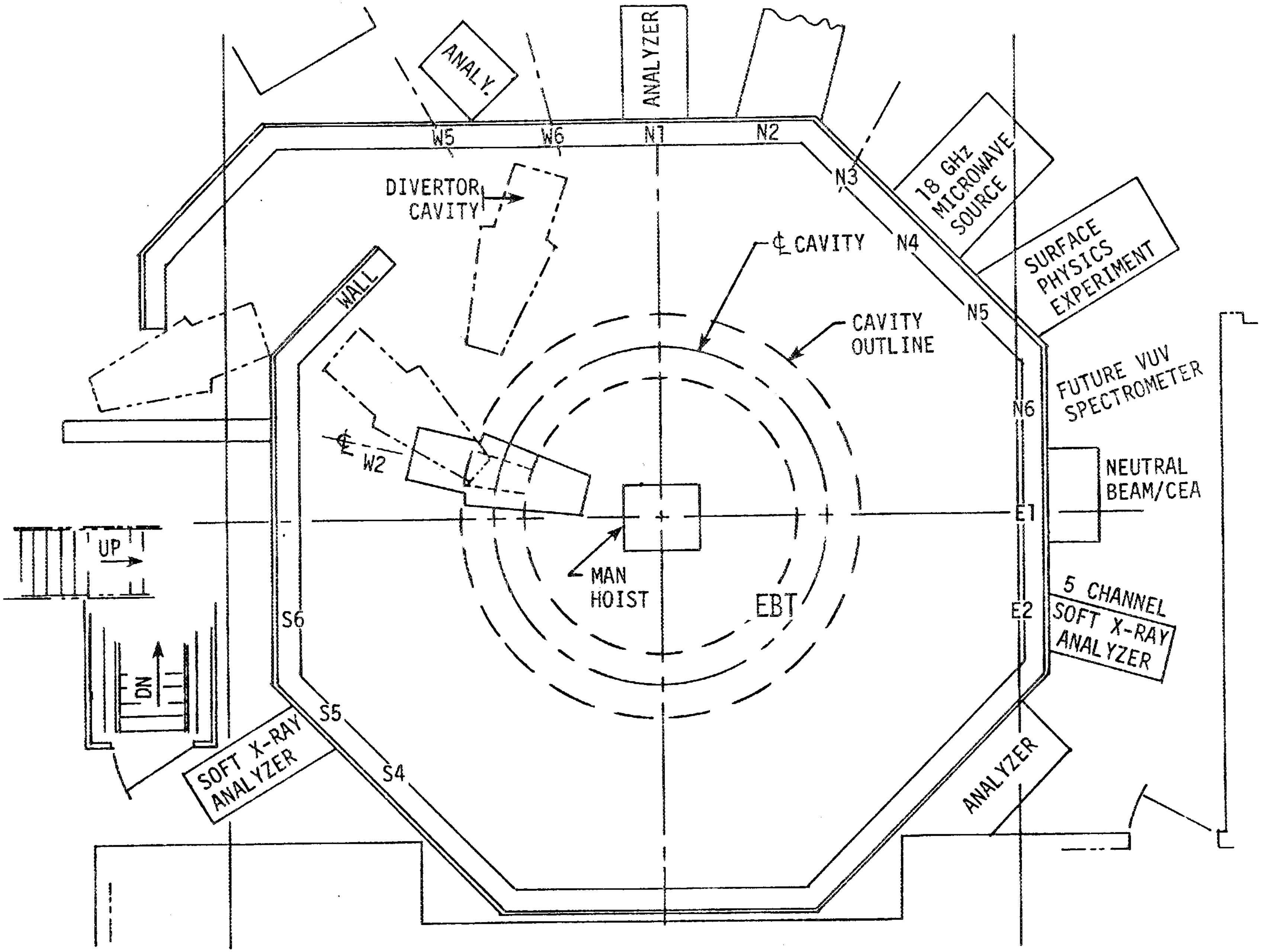

Figure 2-1. Plan View which Shows how the Divertor Cavity, with its Two Adjacent Mirror Coils, can be moved into the Opening in the Torus

are favored because the divertor in any of these locations is between two of the four electrical groupings of the mirror coils. Therefore, routing a mirror coil electrical bus around the divertor is not required. This can be seen in Figure 2-2 which shows that the divertor is located between the ends of mirror coil electrical buses. Also, with the divertor in one of the number 2 locations it is not necessary to cut off one of the vertical torus support posts that carry cooling water to the mirror coils. Figure 2-2 shows the location of the wet and dry support posts.

The divertor cavity is a right circular cylinder. The side toward the center of the torus is wedge shaped, bounded by two side planes. The line of intersection between the end of the right cylinder and the wedge plane is shown in Figure 2-3. This wedge shape conveniently provides clearance between the side of the cavity and the bellows tube between the adjacent standard cavity and the pumping ring. A reasonable design for the turbopump adapter tube is also possible with this shape.

The most serious restraint on the design of the divertor cavity is the requirement that the vacuum pumping ring which also brings microwave power to the cavities cannot be notched or diverted. Therefore, the divertor cavity has to be notched to clear the pumping ring as shown in Figure 2-3. This figure also shows that the divertor cavity rests directly on the unmodified concrete curb. It will be secured to the curb by means of a mounting plate. The two dry torus support posts are cut off flush with the upper surface of the curb.

The width of the divertor on the outside of the torus is based on a compromise between the desire to have space for the installation of vacuum pumping panels for high speed pumping as an upgrade and the need to provide space between the divertor and the adjacent standard cavity so that the plastic coolant tubes from the mirror coils can be brought out. The mirror coil coolant tubes are shown in Figure 2-2.

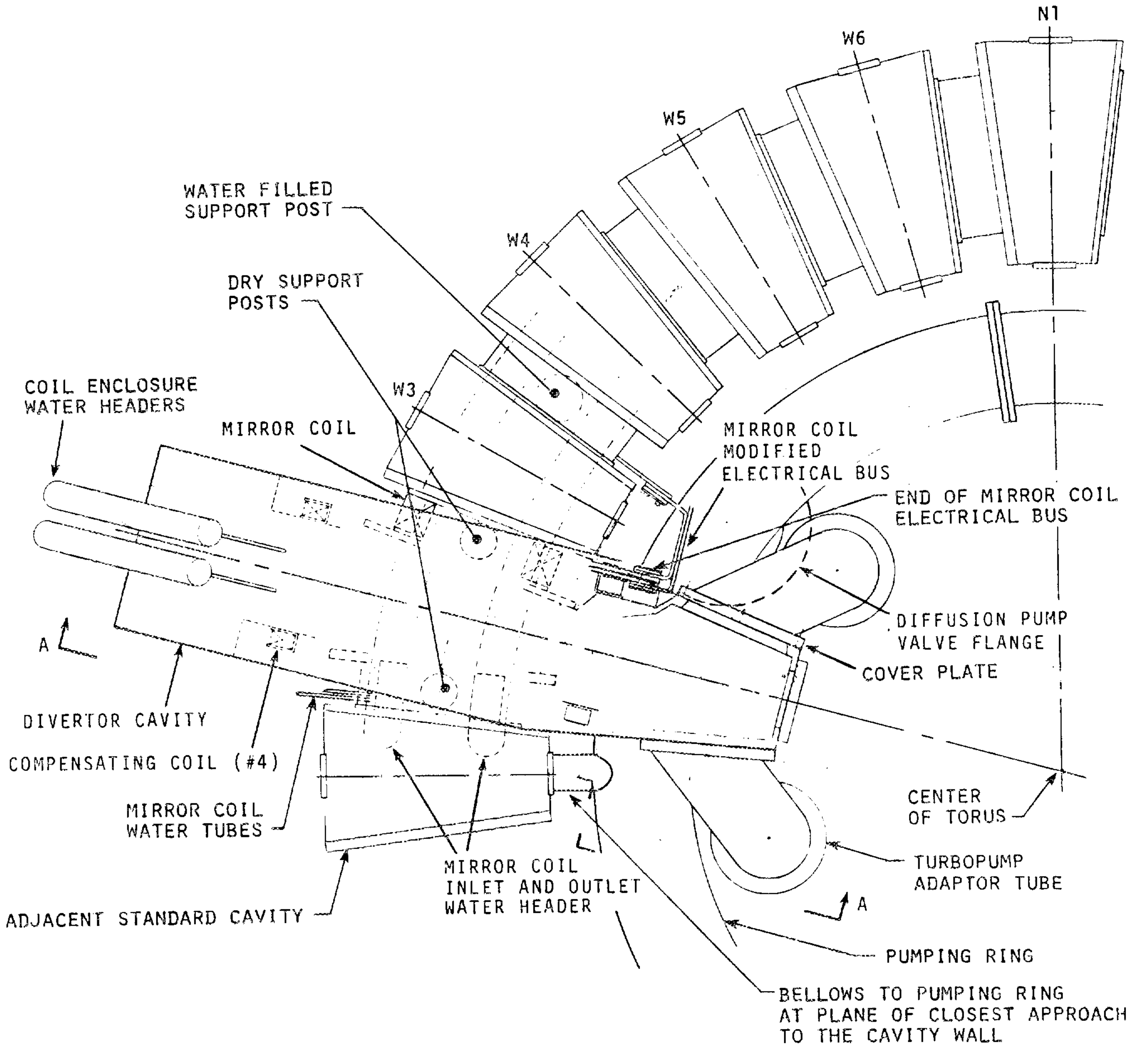

Figure 2-2. Plan View of Divertor with Pumping Panels Showing Interfaces with the Existing EBT-S

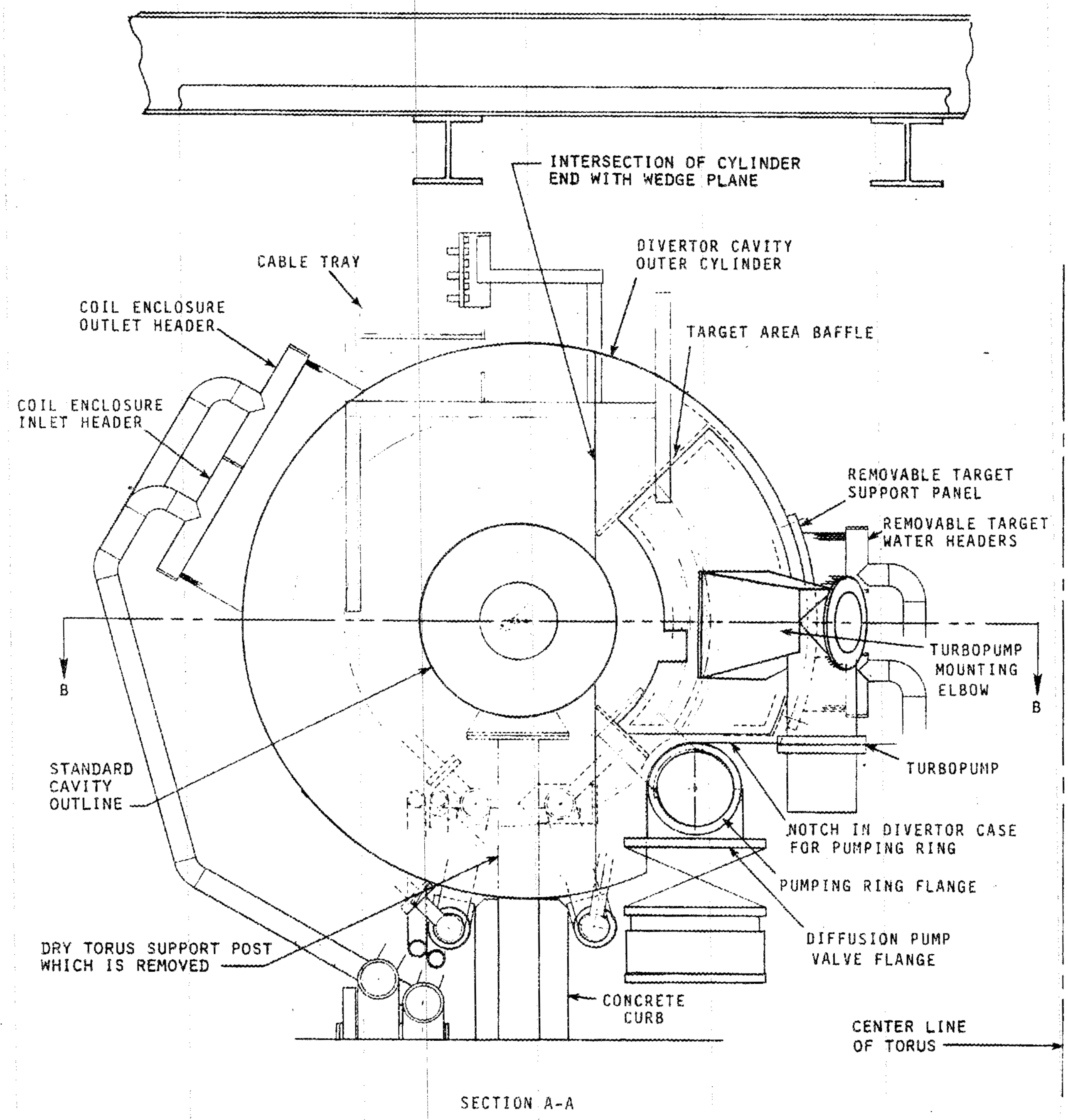

Figure 2-3. Elevation View of Divertor on Section A-A of Figure 2-2 showing the Interfaces with the Existing EBT-S

2.2 DIVERTOR GENERAL ARRANGEMENT

The arrangement of the internal components of the divertor is illustrated in the horizontal cross section drawing of Figure 2-4. (This figure is shown here for convenience; it is the same as Figure 1-3.) The divertor assembly is made up of five major subassemblies; the divertor coil assembly, the divertor cavity assembly, the removeable target assembly, the turbopump assembly, and the mirror coil assembly. The mirror coils are the present EBT-S coils slightly modified, and are considered to be part of the divertor assembly because they must be in place on the sides of the divertor when it is installed into the torus.

The divertor coil assembly consists of the divertor coil enclosure and everything inside. When separated from the rest of the assembly, it will look like a large washer. The two coil support rings form the basic mechanical structure. Coils #2 and #3 are clamped between the two rings and the two halves of Coil #1 are clamped into slots on the outer surface of the ring by the coil enclosure halves.

The divertor coil enclosure, which completely encloses the divertor coil assembly, has four functions: it provides the desired contour for the inside walls of the particle channels; it serves as the cooled target surface for the particle flux for all areas outside the baffle sector; it provides a vacuum containment surface; and it protects the coils from damage should the particle fluxes in a fault situation impinge on the coil enclosure in some area other than the intended target.

The coil enclosure is made up of two copper washers that fit snugly over the coil support rings. These washers have a smooth surface on the outside along the particle channels but are cooled by water tubes attached to the inside. They are capable of absorbing the power density of any normal or fault particle fluxes anywhere on the surface. The two coil enclosure washers are seal welded together at their intersection in the coil throat. The entire divertor coil assembly is then potted with an epoxy resin so that all

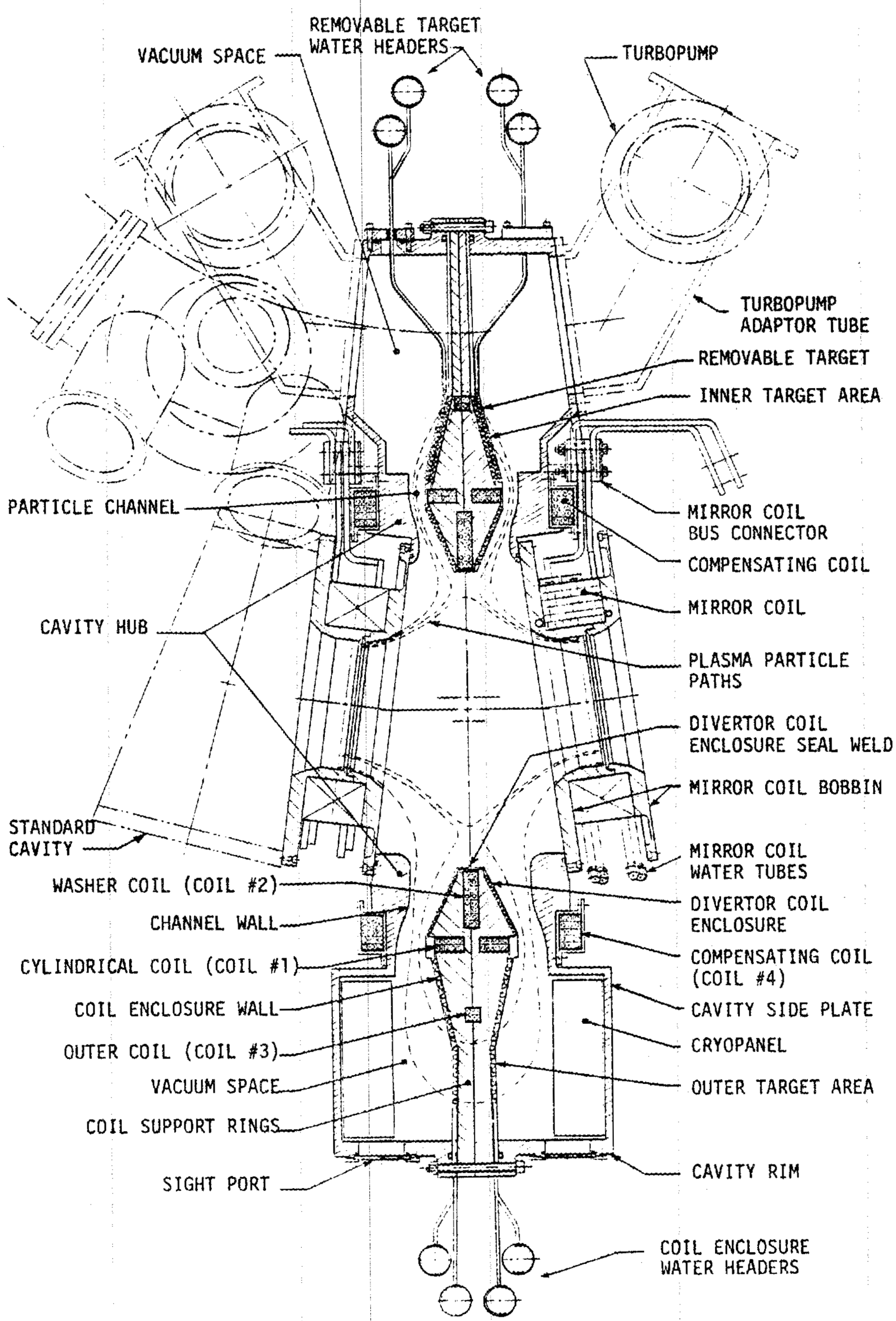

Figure 2-4. Horizontal Cross Section Through the Toroidal Divertor Assembly

interstices around the coils and between the coil support rings and the coil enclosure are completely filled to form a solid unit. The potting is necessary to prevent the atmospheric air pressure from getting between the coil enclosure and the support rings where it would deflect the thin coil enclosure wall out into the cavity vacuum.

The divertor cavity assembly consists of two identical dish-shaped halves that are bolted together at their outer periphery over the divertor coil assembly to form a vacuum container. The cavity assembly is made up of the cavity hubs, the cavity side plates, the cavity rim, and the compensating coils. These components, excluding the coils, are welded together to form a single unit. The cavity rim rests on the concrete curb and supports the entire divertor assembly. The mirror coil bobbins are sealed to the cavity hubs with "O" rings in exactly the same way that they were originally sealed to the standard cavity which has now been replaced by the divertor cavity. The right hand mirror coil of Figure 2-4, previously supported by a support post, is now held by the cavity hub. The left hand mirror coil is supported on its non-flexible bobbin side by a bracket that is attached to the cavity side plate. In this way the mirror coils are supported so that the mirror coil diaphragms are free to flex as needed to accommodate the mechanical tolerances.

The removeable target assembly is a water cooled 90° sector which overlaps the divertor coil enclosure surface in the area toward the center of the torus. It is inserted into position through an elongated slot in the cavity rim. The target is supported by the slot cover plate which is sealed to the cavity rim with an "O" ring. Approximatey 80% of the total particle power is expected to be deposited in this area so that the target will be subject to serious erosion. By making this target surface replaceable without disassembling the divertor cavity, a great deal of maintenance time can be saved.

The turbopump assembly is made up of the turbopump adaptor tube and the Model TMP-1500 Turbomolecular pump manufactured by Leybold-Heraeus Vacuum Products, Inc. (or equivalent). Since this pump is operated with its axis vertical, the adaptor tube is essentially an elbow. This elbow is supported by a cover plate which fits over the opening in the side of the cavity assembly and which is sealed with an O-ring.

The mirror coil assembly is the present EBT-S mirror coil with coil electrical leads that have been shortened and bent to fit around the compensating coil.

2.3 DESIGN OF DIVERTOR COILS

In Phase I of this study, preliminary magnetic design concepts for a toroidal divertor were developed. The present coil configuration is basically unchanged.

Figure 1-2 is a computer visualization of the toroidal divertor coil arrangement showing the relative location of the various coil assemblies (note that no leads are shown for these coils). Ideally, the coils would have very many turns of small wire, with each lead carrying a very small current and thus producing a negligible flux perturbation. Cooling such a coil with the high current densities involved would be impractical; for that reason large conductors with practical coolant ducts are required. A horizontal cross section through the divertor assembly is shown in Figure 1-3. A complete description of the present design philosophy follows.

The coils producing the magnetic field to divert plasma particles to an appropriate target must be designed to meet a number of performance criteria, which include the following:

- The origin of the separatrix or null field point must have a specified location at the edge of the plasma and be external to the coils producing it.

- The flux lines governing the trajectory of the diverted plasma must be directed to a target or sink at a preferred location.

- The flux density at the target must be controlled in order to control the density of energy deposited on the surface of the target.

The location of idealized divertor coil conductors, their cross section, and their current density are parameters requiring close control; deviations in any of the parameters may be cause for serious concern if the diverted plasma misses the target and falls on regions removed from the appropriate target area.

Once the locations of the several divertor coils have been established, adjustment of the null point, target location, and flux density at the target can be accomplished by making simultaneous changes in the currents in the several divertor coils. See Appendix I for a systematic method of adjusting the magnetic field configuration.

Multi-turn coils may consist of a number of pancake layers, a number of cylindrical layers, or some combination of parallel and concentric conductor groupings. For the purpose of discussing magnetic perturbations occuring in coils with optional construction features, a single pancake and a single cylinder with radially extending leads will be considered.

If a single pancake were to be wound with a spiral configuration, the spiral would everywhere provide a local radial current vector component. Nearby field points would sense a field derived from an ideal winding, the weak radial currents, and a perturbation dependent to a large degree on the distance between the field point and the lead that runs from the inner radius of the coil to the outer radius of the coil. The lead-to-field point distance varies continuously with the angular location of the field point. The innermost lead which must be brought out radially past the spiral gives rise to unwanted fluxes. The spiral pancake is thus found to have objectionable features. To circumvent the objections, it is proposed that pancake windings be made of concentric turns to the extent possible. The connection between turns would be an "offset ramp" that allows the conductor at the end of a circular turn to rise up over the start of that turn (for the simple reason that two turns cannot occupy the same space). Each succeeding turn is terminated in a ramp, and if each ramp can be short, the group of ramps will be concentrated in a relatively short span of the circumference. If the inner lead is made to pass the region occupied by the several ramps, the radial current component of the lead will tend to cancel the radial component of the current in the ramps. The circumferential current component will be a substitute for the missing circumferential arcs of current between the starting location of the first turn and the terminus of the final turn; the circumferential distance is that occupied by the group of ramps.

A single layer cylindrical coil could be made with a helical conductor but this too has a continuous axial current component and a concentrated axial lead current if the leads are brought out in close proximity to each other to make them noninductive. In a helix with N turns, the helical lead causes the overall length of the coil to be (N + 1) conductor widths long or one conductor width greater than the nominal coil length. For the cylindrical coil the application of an "axial offset" will provide circular turns without an axial drift component except locally at each offset or the counterpart of the ramp of the pancake coil. One or both leads should follow the "offset line" to obtain as nearly as possible a perturbation-free field.

On the assumption that the perturbations are second order effects, the coils, as described, should be satisfactory. If, however, the perturbations resulting from the design approach described above are excessive, several refinements are possible, such as:

- Split in half the leads that pass over the ramp or offsets, passing half of the current on each of the two coil sides.

- Reduce the ramp or offset length by cutting the conductor at the ends of each 360° arc, plug the ends, and braze successive turns with as short an overlap as possible, with water passed through holes in the sides of the conductors where they are brazed together.

- Add coils near the offsets and leads in order to compensate for the perturbations.

With each additional order of refinement, the residual perturbation should be diminished, but the field can never be perfect. It is necessary only that the residual values be acceptable.

The offset or ramp referred to above can be provided by several means as illustrated in Figure 2-5. The EBT-S Divertor Coils have been layed out on the assumption that the gradual offset will prove satisfactory. With this offset the manufacture will be greatly facilitated since only one offset tool will be required. Details of the various coils are discussed short of explicit instructions for drafting and manufacture.

2.3.1 COIL No. 1 (Figure 2-6)

This coil, normally a 16 turn coil, is to be made in halves. Each half has two layers with four turns each. The inner layer has three axial offsets at the end of turns 1, 2, and 3. The fourth turn terminates in a ramp leading to the second layer. Three additional offsets occur in the second layer. The final lead is brought out radially after it is ramped up out of the second layer where it can be routed along the coil surface following the visible offset path of the top layer and the hidden offset path of the bottom layer. At the end of the route along the coil surface, both leads will be in close proximity and they can be brought out noninductively with very little tendency to produce flux perturbations. Water connections will be required for each electrical turn. The water tube may have double the area of the conductor hole, and since the water tube carries no current it can have a thin wall. An optional arrangement would be to have a pair of these water tubes, each with an area equal to the area of the hole in the conductor. The water connection may be made with a transition piece to connect the exit hole in the side of

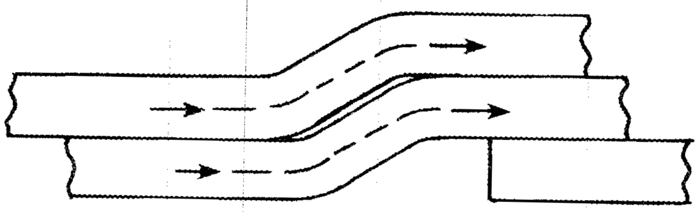

a) Gradual Offset for Continuous Conductors - This Requires No Metal Joining

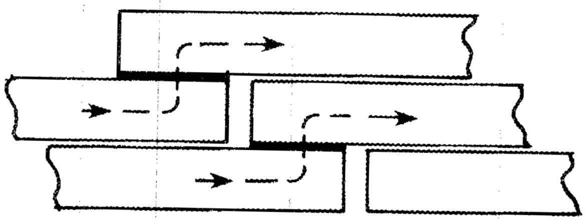

(b) Sudden Offset with Square Ends. Brazing or Other Joining Processes are Required Including Plugging of the Conductor Ends. Holes Through Joint Required for Coolant

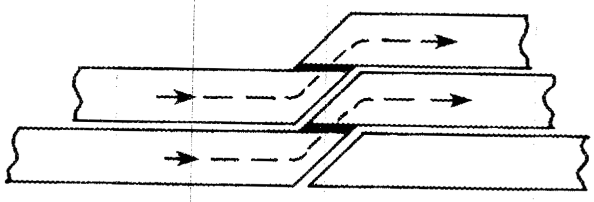

c) Mitered Offset for Least Possible Circumferential Current Disturbances

Figure 2-5. Options for Conductor Turn-to-Turn Transitions in Coils

383F/J56

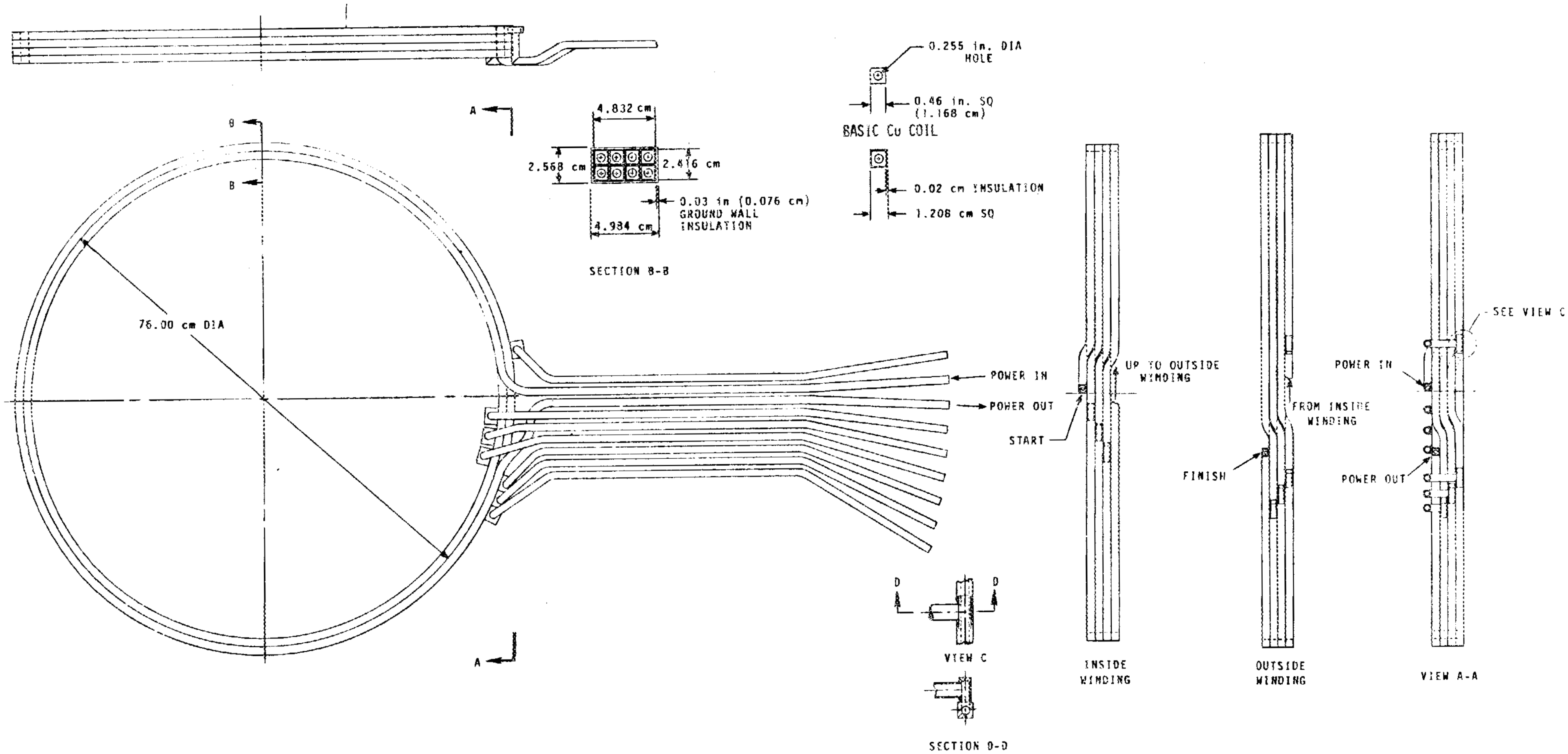

Figure 2-6. Coil and Lead Configuration of Coil #1, the Main Divertor Coil

the conductor with the thin-walled water-carrying tube or tubes. The water tubes for all of the coils must be insulated from each other, from ground potential, and all other leads.

2.3.2 COIL NO. 2 (Figure 2-7)

This coil, as shown, consists of two pancakes placed back-to-back at the midplane of the divertor. The No. 2 Coil leads and water tubes will pass radially between the halves of Coil No. 1. Each pancake has eight circular turns with ramps between turns. The inner lead will follow the group ramp line to the second or outer lead, from there both leads will be brought out together. Each water circuit will have four series turns; water connections must be located halfway between the leads. The single thin walled water tube to each pancake may either supply or carry away all of the water for that pancake. If space limitations crowd the leads where they are connected to the innermost turns, a modification may be in order. Rather than put two eight turn pancakes back-to-back, it may be advantageous to make one eight-turn circuit of a single continuous conductor that is wound to have two turns in one layer and six in the other. The second circuit would consist of eight turns having a reverse winding with six turns outside of and completing the layer with two turns, and with two turns outside of and completing the layer with six turns. The second set of eight turns will not be easily wound from a single conductor and the continuous eight turns must be achieved by connecting the last turn of each layer both electrically and hydraulicaly. Leads and water connections would now be located at least two turns removed from the innermost turn and as a consequence would not be as crowded. No electrical function would be sacrificed.

2.3.3 COIL NO. 3 (Figure 2-8)

This coil has four turns, with two conductors paralleled electrically. The coil has been formed by: stacking two conductors radially, forming a full circle with the conductor pair, offsetting both conductors axially, completing the second turn, and bringing out the leads. No special routing of leads is

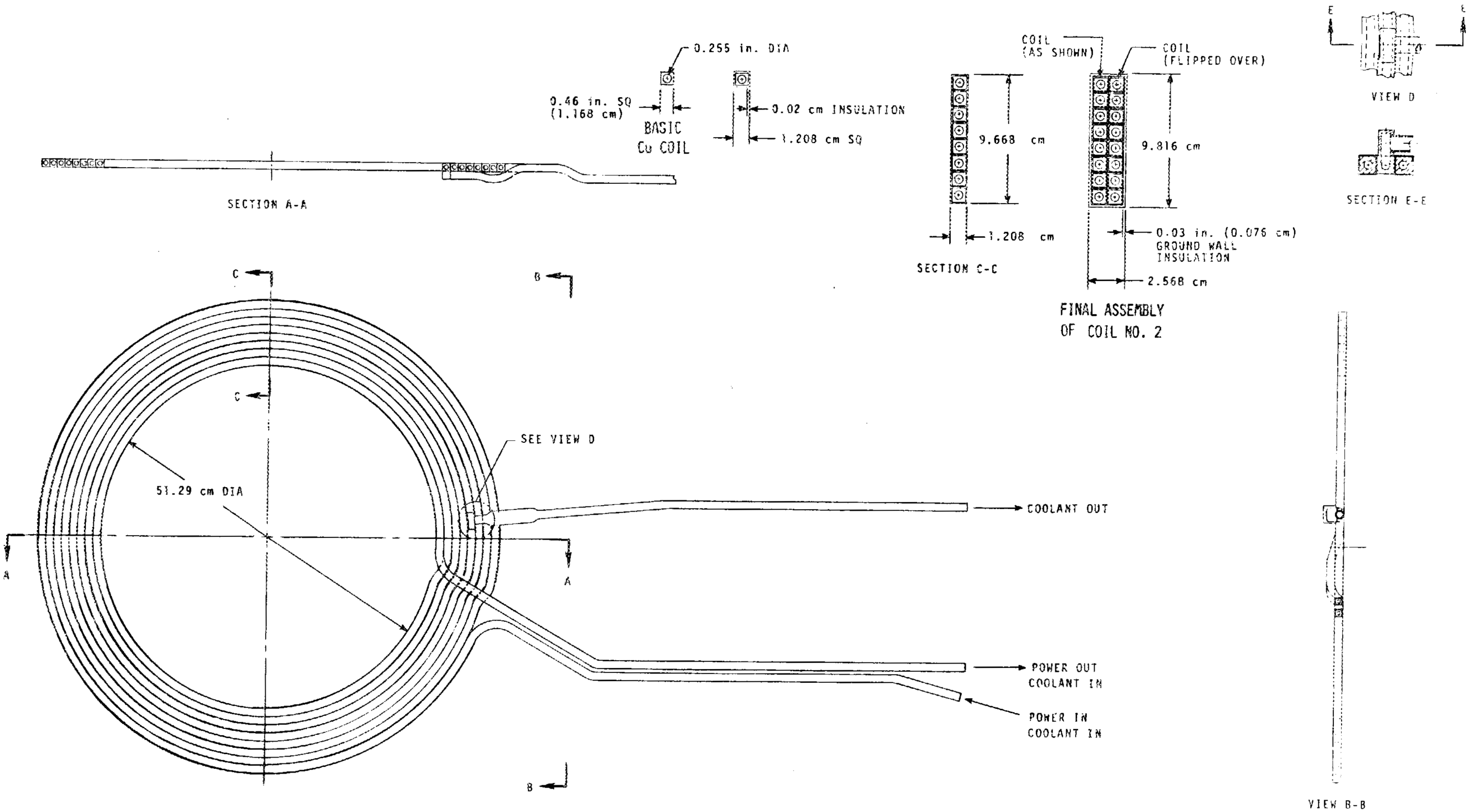

Figure 2-7. Coil and Lead Configuration of Coil #2, one of the Main Divertor Pancake Coils

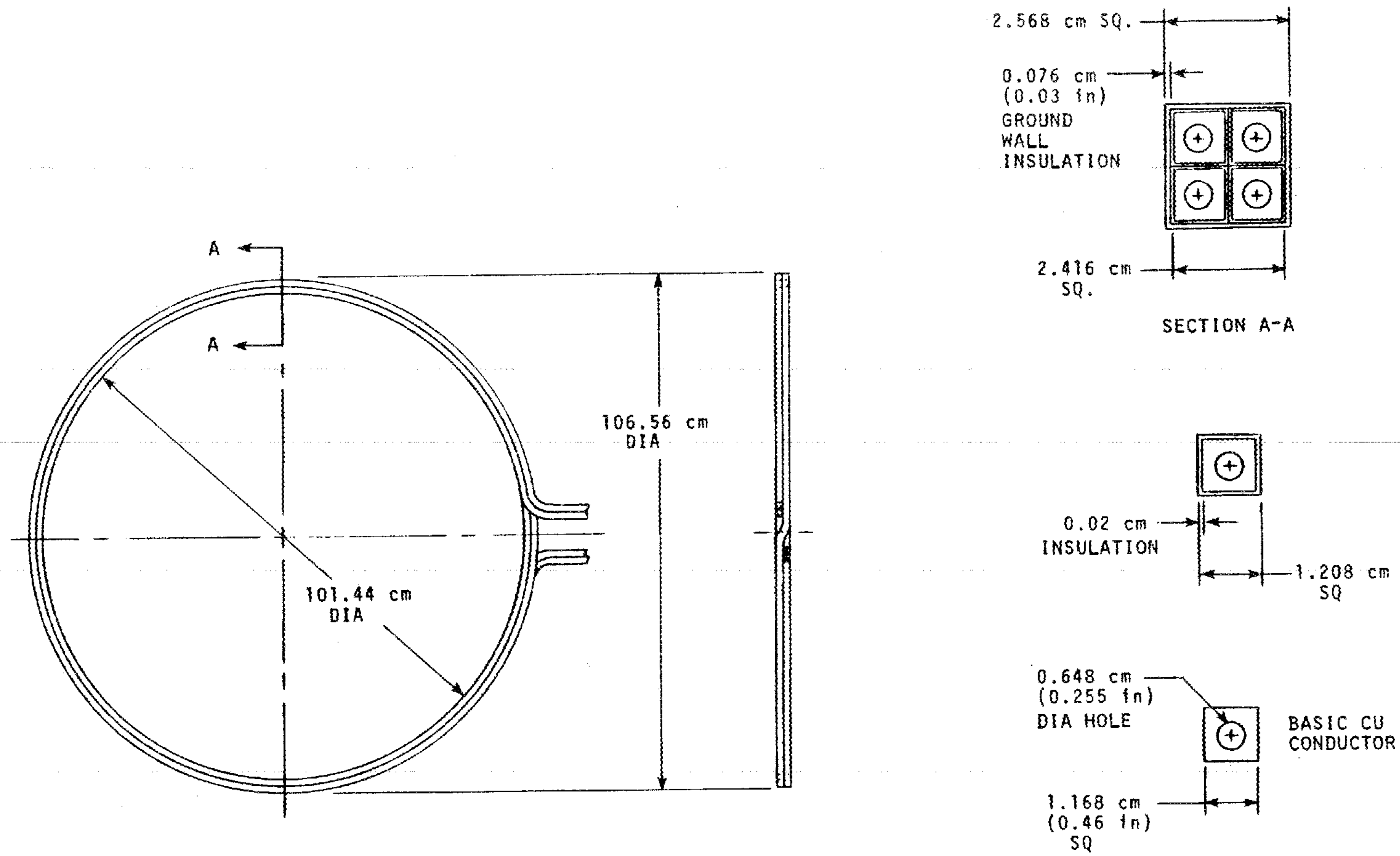

Figure 2-8. Conductor and Lead Configuration for Coil #3, the Outermost Divertor Coil

required other than making certain that the leads be brought out close to each other. Water will enter one lead pair and leave by the other.

2.3.4 COIL NO. 4 (Figure 2-9)

The compensating coils are located externally with respect to the vacuum enclosure. Each of the compensating coils has 15 turns arranged as five, three-turn layers, and for that reason some special considerations are necessary.

The first and second turns in each layer terminate with an axial offset to the next turn, while the third turn terminates in a ramp to the next layer. The offset paths are buried within the five layers and it is proposed to compensate for 14 offsets (radial and axial combined) by carrying the internal leads around the coil surface until the leads meet. In this case a sudden offset, or a mitered offset, should prove to be very useful in minimizing the production of unwanted fluxes, but only as a last resort as far as manufacture is concerned.

The winding requires one water circuit per turn, but the principal location for water connections is conceived as being on the faces of the outer five-turn coil groups. It is a matter of interest that the five hidden turns in the middle of the coil may be reached by way of water connections at the outer five-turn faces. There are five starting ends and five finish ends visible on each face. There are two ramps visible on each five-turn face, five ends that are connected to the inside group of coils by means of the axial offsets, and one free end or electrical lead. With eight water connections on each face there are sixteen connections to carry water to or from the fifteen-turn coil. Each turn will be cooled with its own water circuit. The inner turns are each accessed directly by way of the axial offset within a portion of the circumferential offset length which can be seen next to the ramps. It can be seen in Figure 2-9 that all coil faces have been utilized to achieve the cooling requirements mentioned above.

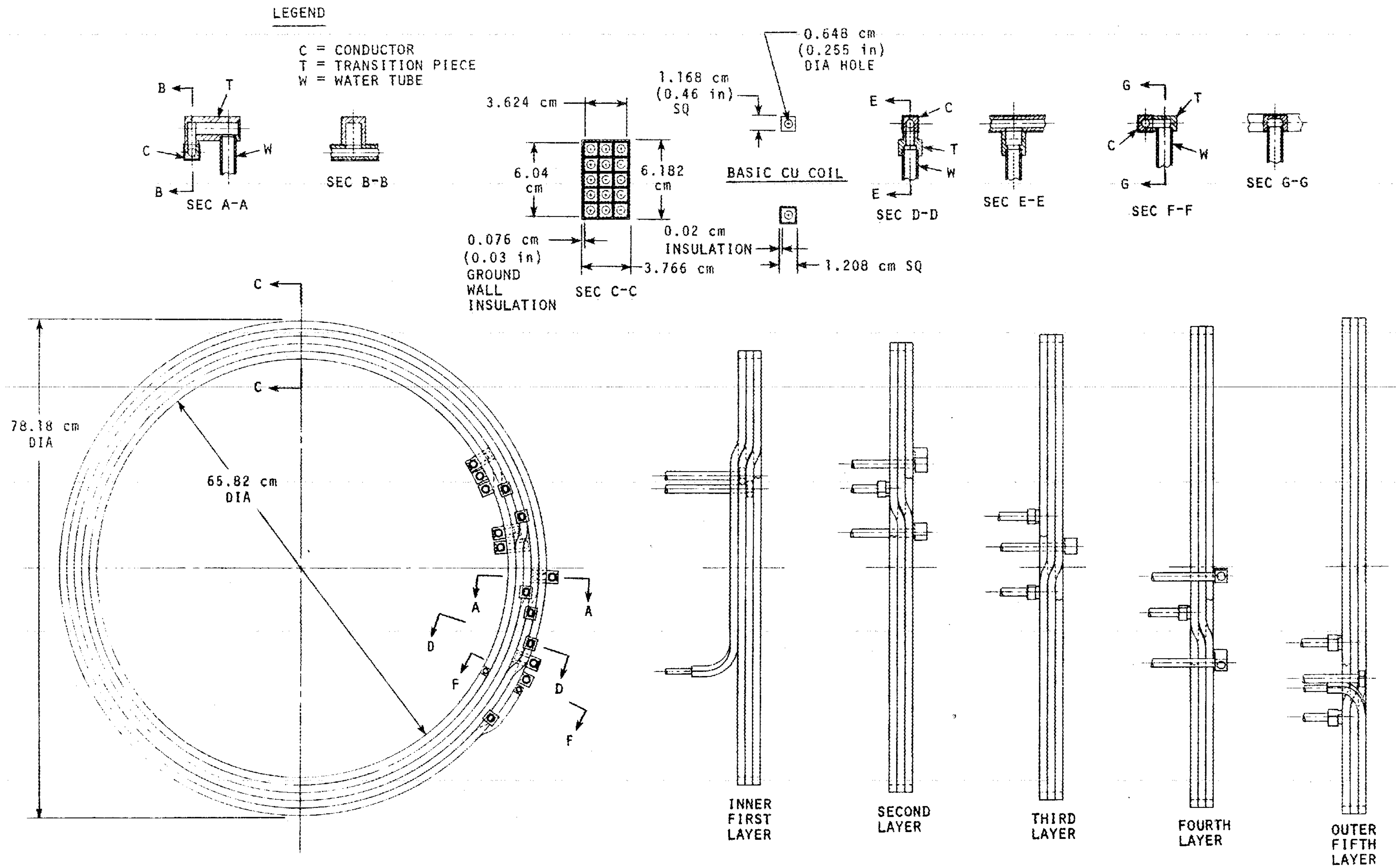

Figure 2-9. Coil and Lead Configuration of Coil #4, a Divertor Compensating Coil

2.3.5 ELECTRICAL CIRCUIT FOR THE DIVERTOR COILS

The conductor for each of the divertor coils is a common commercial square conductor, 1.168 cm (0.46") on a side with an 0.6477 cm (0.255") round hole for water cooling. The common size conductor was chosen to very nearly occupy the available design space when each coil is pictured as an ideal single turn coil having a uniform but unique current density which is required to generate the desired divertor flux. Since it is proposed to operate all coils in series, it might appear desirable to tailor the number of turns in each coil to more nearly equalize the currents in the several coils, but such a modification would require too many conductor sizes rendering a single conductor section impractical. Even then it would be unlikely that the currents would match exactly. The ampere ratings of appropriate coils having an identical conductor cross section vary from 3000 to 7893 amperes. If certain coils have two parallel conductors acting as one, the current ratings will be 7893 amperes, 7500 amperes, 6600 amperes, and 6000 amperes, respectively, for Coils #1 to #4.

It is proposed that all coils should be connected in series and that coils with less than the greatest ampere rating have a resistance shunt across their terminals. The shunt will be designed to bypass just enough current that the coil current plus shunt current will equal the current in the coil with the greatest ampere rating. Each coil, whether shunted or not, will have an auxiliary power supply shunted across its terminals. When the power supply voltage matches the voltage across the shunted coil terminals, there will be no flow of current to either boost or buck the current in the coil. If an adjustment is desired the power shunt may boost the current a few percent (5% assumed) by drawing energy from the power grid, rectifying it, and delivering it to the shunted coil. To obtain a full range of fine current trimming it may be necessary to employ a coarse shunt adjustment to bypass slightly more current than desired. The auxiliary power shunt would always be used for fine adjustments.

Since all coils are connected in series, they may be excited by a common power source. The sum of all coil voltages will be under 200 volts so that it will be possible to use an existing 3 MW dc generator rated at 350 volts to excite all divertor coils simultaneously. Coarse control of individual coils can be accomplished with variable resistance shunts across the coils; fine control can be obtained by the use of auxiliary power shunts. Figure 2-10 illustrates a possible circuit arrangement.

2.3.6 WATER COOLING OF THE DIVERTOR COILS

The proposed divertor coils will be wound from a continuous length of square copper, 1.168 x 1.168 cm, with an 0.6477 cm round hole for water cooling. Because of the difficulty in circulating water from one end of a coil to the other, the coil length will be divided into a number of equal smaller lengths and holes will be provided through the conductor sides so that any preferred number of turns per water circuit may be realized. The turns per circuit may even be fractional if it is found desirable for the sake of limiting velocity or pressure to circulate the cooling water.

Table 2-1 summarizes the data relative to the cooling requirements. Note that all coils will be connected in series and for that reason the design currents were selected to be nearly equal to each other. Current differences are recognized and shunts across coils will accommodate the differences.

The divertor coils together require 6.9 liters per second or 414 liters per minute of water (this corresponds to 109 gallons per minute). The water pressure required is no more than 446 kPa or 65 psi and it would be well to use a flow meter in each coil water header to regulate flow. The overall energy consumption is 1.37 MW. The power supply is a 3 MW dc generator rated at 350 volts and 8571 amperes. The available current is 8.5% greater than the calculated demand and the voltage margin is greater still.

The water cooling calculations were based on an assumed ambient water supply temperature of 30°C and a maximum conductor temperature of 95°C. The estimate

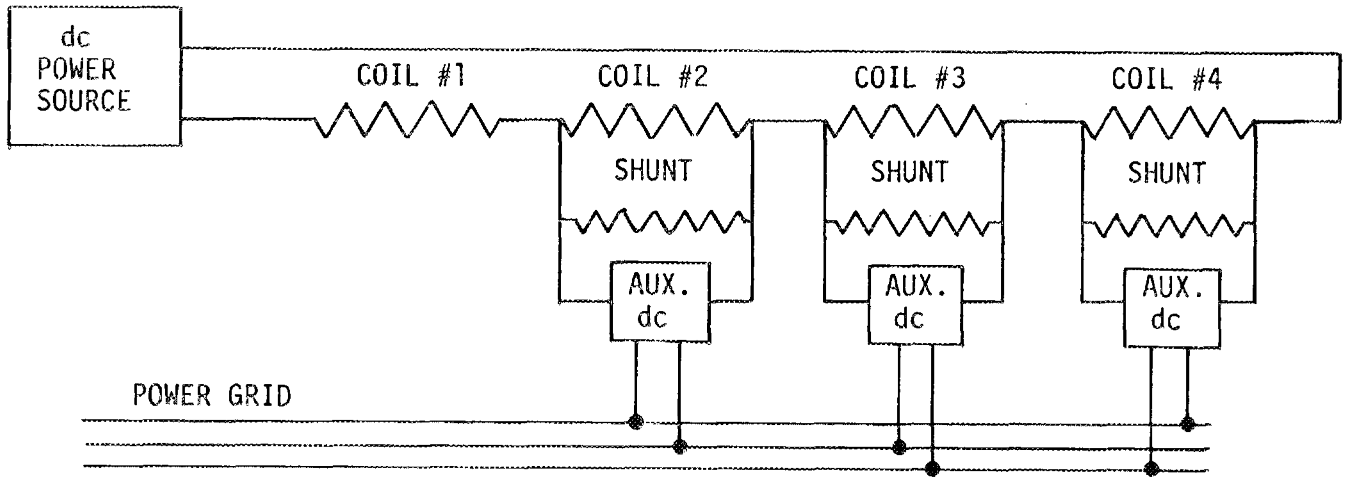

Proposed series connection for all coils

- o Coil voltages may all be different
- o Shunts may all be different
- o Auxiliary dc supplies may all be different
- o Auxiliary dc unit ratings may be considerably reduced if shunts are variable
- o Power source: an existing three MW dc generator rated at 350 volts

Figure 2-10. Schematic Representation of the Proposed Divertor Coil Excitation Approach

TABLE 2-1

DIVERTOR COIL CURRENT, LOSS, AND WATER COOLING DATA

COIL NUMBER	1	2	3	4	OVERALL DIVERTOR CHARACTERISTICS
TOTAL TURNS (Conductor Loops)	16*	16	4	30**	
CURRENT/CONDUCTOR, A	7893	3750	3000	6600	7893[a]
CONNECTION TYPE	SERIES	PAR.+	PAR.+	SERIES	
TERMINAL CURRENT, A	7893	7500	6000	6600	
LOSS PER WATER CIRCUIT++, kW	36.6	23.3	12.9	21.3	
NUMBER WATER CIRCUITS	16	4	2	30	
LOSS/COIL, kW	509	93.3	25.8	605	1365[b]
COIL VOLTAGE, V	64.5	12.4	4.3	91.8	173[c]
CIRCUIT FLOW RATE, kg/s	0.190	0.096	0.053	0.112	
COIL FLOW RATE, kg/s	3.05	0.384	0.106	3.36	6.9[d]
FLOW VELOCITY, m/s	5.78[e]	2.91	1.61	3.40	
CIRCUIT PRESSURE DROP, kPa	446[f]	289	27.7	126	

* Two half coils of eight turns, each connected in series

** Two distinct compensating coils with fifteen turns each

\+ Two conductors in parallel acting as one electrically but providing two water circuits

++ Loss per water circuit including lead or leads for most adverse circuit. Note that some water circuits have no external electrical leads, hence loss per circuit multiplied by circuits does not always give loss per coil

a All coils connected in series with maximum current (7893 A) in circuit.

b Although individual losses total 1273 kW, the sum of 1365 kW is delivered from the power supply, with the extra 132 kW going to the shunts across the coils.

c This is the calculated sum of the coil voltages in series.

d This is water to coils, neglecting losses in shunts which could be air cooled.

e This is the maximum flow velocity. If a fractional turn per circuit were used the velocity could be reduced.

f This is the greatest needed pressure. All coils should have flow control to regulate the water flow in each coil.

of maximum temperature at the end of the cooling circuit included the following considerations:

Ambient Water Temperature
Water Temperature Rise
Surface Film Temperature Drop
Internal Temperature Difference Within the Conductor.

It is believed that the available water supply for cooling the coils is more than adequate and that if water flow is controlled to give more than the indicated flow in Table 2-1, the coils can operate with a reasonable margin with respect to the maximum allowable copper and insulation temperature, which can be set at something less than the 95°C used in establishing Table 2-1.

2.3.7 X-RAY DOSE TO COIL INSULATION

The divertor coil insulation is assumed to be glass tape treated with a B-stage epoxy resin or untreated tape which is subsequently impregnated with resin.

In the design that has been described, the main divertor coils will be potted inside the coil housing to avoid having air at atmospheric pressure acting on one side of a wall that faces a vacuum on the other side. The potting resin may also serve as the coil insulation impregnant.

The radiation resistance of impregnated glass tape is largely dependent on the choice of resin and the curing agent. One candidate resin is DER332LC with either epoxy curing agent Z or agent MPDA and MDA. This resin is available from Dow Chemical in Freeport, Texas. The radiation resistance of glass and DER332LC is[4]:

2.5×10^{9} rads for threshold degradation
2.65×10^{10} rads for 25% degradation
7.4×10^{10} rads for 50% degradation
2.0×10^{11} rads for 90% degradation

The x-ray production in an EBT arises primarily from the scattering of energetic electrons which have been created in the stabilizing annuli and their subsequent escape and impingement on solid surfaces. At this time, there is much uncertainty regarding the fate of these electrons should a divertor be energized. To a large extent, their history will depend on the operating conditions, i.e., the location of the electron rings relative to the scrape-off layer. A large fraction of the electrons, particularly those located on flux lines that do not intercept the target area at the time of scattering into a loss cone, should share their energy with the bulk plasma prior to entering a divertor chamber. It is assumed that one half of the energetic electrons are promptly diverted to the divertor chambers without loss of energy where they impinge uniformly in the poloidal direction on the two targets.

For 28 GHz operation, it is assumed that the temperature of the electrons in the rings is 500 keV and that the field at the rings is 0.5 T. As upper limits it is further assumed that the electron ring density is 3×10^{17} m^{-3}, the density of the background ions at the rings is 4×10^{18} m^{-3}, and the total volume of the electron rings is 0.08 m^3. These assumptions result in a total power loss from all the rings of ≈10 kW. This result is based on analytic expressions[5] and includes synchrotron radiation, bremsstrahlung radiation, scattering on background ions into the loss cones, and drag on the background electrons. (Based on more likely conditions, viz, an electron ring density of 2.5×10^{17} m^{-3}, a background ion density of 1×10^{18} m^{-3} and a total ring volume of 0.04 m^{-3}, the total power loss from the rings would be an order of magnitude smaller.)

The energetic electrons which escape from the rings via scattering represent ≈10% of the total power loss. Therefore, <1 kW of energetic electrons escape, and <0.5 kW create energetic x-rays in the divertor chambers. For an electron temperature of 500 keV and a tungsten target, ≈10% of the energy associated with the electrons is converted to x-rays. Therefore, <50 W of x-rays would be produced.

The photon flux corresponding to a dose rate of 1 mrem/hr is given by[6] 1 mrem hr^{-1} = 560 E^{-1} photons cm^{-2} s^{-1}, where E is the photon energy in MeV. By definition, one rem corresponds to the absorption in tissue of 87 ergs of radiation per gram, whereas one rad corresponds to the absorption in a material of 100 ergs per gram. Assuming that absorption in the coil insulation is equivalent to absorption in tissue, 1 rad (insulation) = 1.15 rem, and 1 rad (insulation) hr^{-1} = 6.44×10^5 E^{-1} photons cm^{-2} s^{-1}. From this relationship, and under the following assumptions,

- <50 W of x-rays produced by a Maxwellian distribution of electrons with a temperature of 500 keV

- no x-ray shielding

- electrons escape from the rings and impinge on a total of 250 cm^2 of target area before losing any energy

- one half of the photons produced pass into the coils,

it is estimated that locally, where the electrons dump, the dose rate to the coil insulation is $\lesssim 1 \times 10^6$ rads hr^{-1}. If the dose to the insulation is to be limited to 1×10^{10} rads, the insulation could be exposed for >1200 eight-hour days. Because of the low voltages involved (∿200 V), damage to the insulating properties of the material should not be a problem provided the insulation maintains the spacing between conductors. If the dose to the insulation were limited to 1×10^9 rads, the insulation could be exposed for >120 eight-hour days.

No shielding has been provided in the design of this experimental divertor. While some detailed specifications for insulating and potting the coils must be worked out, sufficient data is at hand to assure that coils that can tolerate the existing radiation levels can be produced.

2.3.8 SUMMARY OF FORCES AND TORQUES

The JXB forces on the divertor coils and adjacent mirror coils were calculated for normal operating conditions and for the accident condition where three successive mirror coils on one side of the divertor are not operating. These results and the associated analyses are reported in Reference 3. The coil turning moments have now been analyzed and the results are summarized in this section.

Because of symmetry there will never be any overturning moments tending to rotate any coil about an axis passed horizontally through the plane of the coil nor will there be any moment tending to rotate it about an axis normal to the plane of the coil. The only moments that tend to rotate a coil out of its plane are moments about a vertical axis.

In normal operation the only coils to be subjected to a torque or turning moment would be the mirror coils and the compensating coils. Taken in pairs (one on each side of the divertor), the net moment for the mirror coils attached to the divertor and the compensating coils is zero, and for this case the principal divertor coils are not subject to torques about any axis.

Assuming that three adjacent coils to the divertor are not carrying current, torques will be observed for each of the principal divertor coils, the compensating coils, and the mirror coil that does carry current. To resist the total normal force and twisting moment for any coil, a force equal in magnitude to the normal force could be applied at an offset from the coil center. The offset distance is the distance of the force centroid from the coil center. In all cases, both normal and faulted, the force centroid displacement never exceeds 5 cm and therefore the moments are not sufficiently large to warrant special design consideration. (The maximum torque would be experienced by a mirror coil during normal operation, viz, 650 newton-meters or 480 foot-pounds.) More important than the effect of the moments is the problem of supporting the entire divertor on its foundation.

In normal operation the mirror coils each pull away from the divertor with a force of 13 kN, but these cancel each other. The compensating coils pull away from the divertor with a force of 38 kN and these also cancel each other. Locally then, the "yoke" of the divertor structure must resist a force of 51 kN (11.5 x 10^3 pounds) on each side.

During a fault condition with three adjacent mirror coils on one side of the divertor not energized, the following forces will act normal to the divertor coil plane. For the active mirror coil 24 kN directed away from the divertor. For the adjacent compensating coil 46 kN directed away from the divertor. For the three main divertor coils acting as a whole, the force is 30 kN directed away from the active mirror coil. For the remaining compensating coil adjacent to the inactive faulted mirror coils, the force is 27 kN directed away from the active mirror and the main divertor coils. The active mirror coil and the adjacent compensating coil are acted on by a total force of 70 kN directed away from the divertor and the divertor with the remaining compensating coil have opposing forces of 57 kN. The net force on the assembly consisting of two mirror coils and the divertor will be 13 kN tending to overturn the assembly.

It is of interest to note that the greatest radial force on the divertor tending to pull it toward the major axis occurs during normal operation when the out-of-plane forces are zero. The pull toward the center of the torus is approximately 8000 newtons or 1800 pounds.

In summary, the divertor assembly must be restrained from moving toward the major axis during normal service. Furthermore, if a fault occurs that eliminates excitation in adjacent coils at one side of the divertor there would be a tendency to topple the divertor on its side.

To resist the centering and overturning moments, the base of the divertor will be outfitted with a mounting plate or mounting pads suitable for attachment to the foundation (referred to as the "curb") which must be modified to provide a rigid footing for the divertor mount. This will be in the form of a plate anchored to the curb, which may need in part to be chipped away to make room for the mounting details.

Since the supports for the two mirror coils (now attached to the divertor assembly) will have been removed, the divertor mount must function in their stead. It will be necessary in the final design phase to determine the flexibility of the original hollow post support system and, if necessary, build in an equivalent degree of flexibility so that the divertor mounted mirror coils will respond to the centering forces in concert with the other mirror coils.

2.4 DIVERTOR COIL ENCLOSURE

The details of the design of the coil enclosure, which were described briefly in Section 2.2, are most readily understood by referring to Figure 2-4. The coil enclosure is made up of two water-cooled copper washers machined from copper weldments. The inside diameter of the washer is in the throat of the divertor coil and the outside diameter is the maximum OD of the divertor assembly. The surface contour of the washers could be machined on a lathe face plate to keep down the cost. This can be understood by envisioning the washers to be two identical dinner plates with their upper sides placed face-to-face. If the plates are then separated at one edge by a small amount, the bottoms of the plates will have surfaces related to each other in much the same way as the outer surfaces of the two washers. After the basic machining, each washer is fastened to the face plate with a new axis, set at an angle to the original axis. A facing cut is made at the throat of the washer where the seal weld will be made. The outer surface of each washer shows in the horizontal cross section of Figure 2-4 as a series of straight lines because it is very easy to turn tapers on a lathe compared to turning a surface with a rounded contour. A washer contour that followed the smooth particle path more closely would look better, but it is believed that it would add very little to the performance. The outer surface of the coil enclosure is smooth and polished. If desired, it could be spray coated with a sputter-resistant surface, similar to the targets.

The way that the coil enclosure is water-cooled is illustrated in Figure 2-11. The inner surface is lined with copper tubes 0.65 cm square with a 0.457 cm square hole soldered into grooves machined into the washer inner surface. The machined grooves accurately locate the tubes without the use of any assembly fixtures. Because there is little clearance between the tubes and the groove wall, the solder, by capillary action, will completely fill the gap and provide good thermal contact between the tube and the washer. Since each tube is a single circular loop, these grooves can also be machined on a lathe. This could not be done if the tubes were wound as spirals.

The tube pattern for the coil enclosure is shown in Figure 2-11. Water flows in opposite directions in the adjacent tubes, resulting in a uniform temperature distribution over the surface of the enclosure. Figure 2-11 also shows that the outside diameter of the tube pattern toward the center of the EBT-S torus is fixed by the necessity to clear the notch in the cavity that was cut out for the pumping ring. The outside diameter of the tube pattern must be larger toward the outside of the EBT-S torus in order that the target area will be cooled. The particle flux impingement area can be seen in Figure 2-4. The tubes appear to be spread out at the outside in this figure because each groove is machined with a different center. The reduced heat absorbtion capability of the spread out tubes is acceptable because of the reduced surface power density in this area.

Table 2-2 is a summary of the design shown in Figure 2-11. The water velocity for the outer ring of tubes is higher than for the inner ring even though the design power density is the same because the tubes are more widely spaced in the outer ring. Figure 2-11 shows both the inner ring and the outer ring receiving water from the same header. Because of the difference in pressure required to obtain the flow velocity specified for each of the rings, each of the tubes will be orficed. The ΔP shown is the pressure required to obtain the water velocity in the longest length of tube. The maximum pressure drop which is available at the device is the inlet pressure less the drain back pressure or 160 psi. Since the pressure drop required by the outer ring is only 130 psi, the design is acceptable.

383F/J56

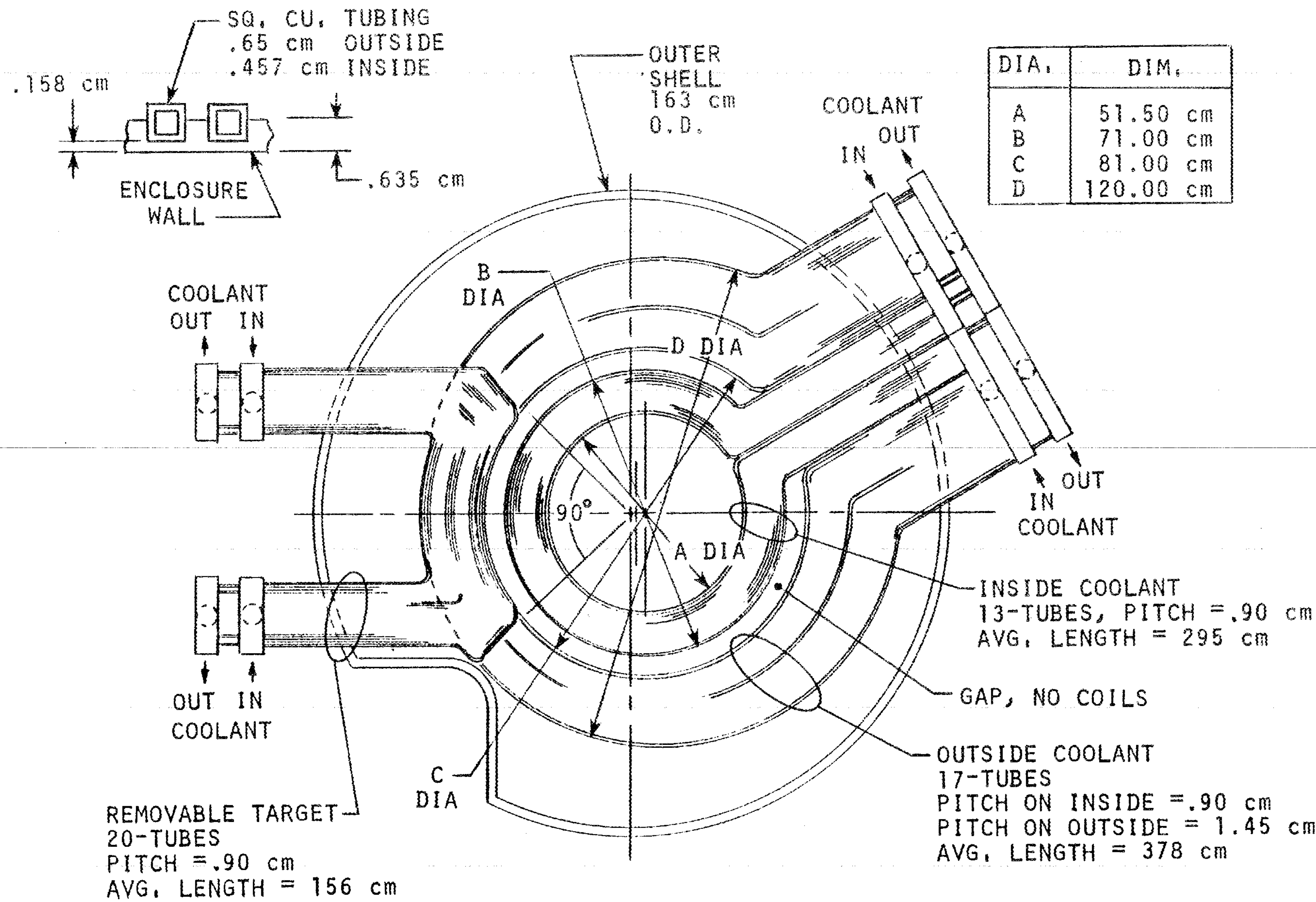

Figure 2-11. Divertor Coil Enclosure Tube Patterns Showing that the Removable Target Overlaps the Coil Enclosure and Showing Water Headers which Provide for Water Flow in Opposite Directions in Adjacent Tubes

TABLE 2-2

SUMMARY OF PARAMETERS FOR THE EBT-S DIVERTOR WATER-COOLING SYSTEM

	REMOVABLE TARGET	COIL ENCLOSURE: INNER RING	OUTER RING
No. of Tubes	20	13	17
Avg. Length of Tube, cm	156	295	378
Longest Length of Tube, cm	181	315	410
Heated Length of Tube, cm	165	307	308
Design Power Density, kW/cm^2	0.22	0.15	0.15
Water Velocity, m/s	5.95	7.39	10.36
Water Flow Rate, kg/s (gpm)	2.36(39)	1.94(32)	3.55(58)
ΔP, MPa (psi)	0.17(24.5)	0.39(56.7)	0.89(129.6)

Water System Inlet Pressure = 1.78 MPa (200 psig)
Water Drain Back Pressure = 0.36 MPa (40 psig)
Water Inlet Temperature = 32.2°C (90°F hot day in summer)
Water Outlet Temperature = 98.9°C (210°F maximum)

Figure 2-4 shows that the coil enclosure washers fit closely over the coil support rings that also extend to the maximum OD of the cavity. An "O" ring in the divertor cavity rim at the outer diameter of the enclosure seals against the polished surface of the coil enclosure to make a vacuum tight cavity.

2.5 REMOVABLE TARGET

The removable target was described briefly in Section 2.2 which referred to Figure 2-4. The general shape of the removable target and the location of the water headers is shown best in the elevation view of Figure 2-11. Figure 2-12 shows the pattern of the tubes in the target in greater detail. It should be noted that the tubes are closely spaced near the horizontal plane where the power density is the greatest. The wider spacing between the tubes where the tubes are bent sharply near the baffles will not cause an excessive surface temperature because the power density is much less in this area. The parameters for the coolant water system have been summarized in Table 2-2.

2.5.1 EROSION OF THE TARGETS

The copper surface of the target will be plasma sprayed with an ∿0.1 mm thick layer of tungsten in accordance with the following analysis. One of the major functions of the divertor system is to minimize the direct interaction of the plasma with the torus walls and to transfer that interaction to the target in the divertor chamber. Arcing and sputtering, both physical and chemical, can erode the target surface limiting its useful life. Also, the atoms eroded from the target surface will tend to deposit in the divertor chamber covering windows and perhaps having a deleterious effect on any getter pumping surfaces, e.g., ZrAl panels. An estimate has been made of the physical sputtering expected from the EBT-S divertor target.

A peak particle flux of 5×10^{17} cm^{-2} s^{-1} and an average particle flux of 1×10^{17} cm^{-2} s^{-1} has been predicted under the following assumptions[3]:

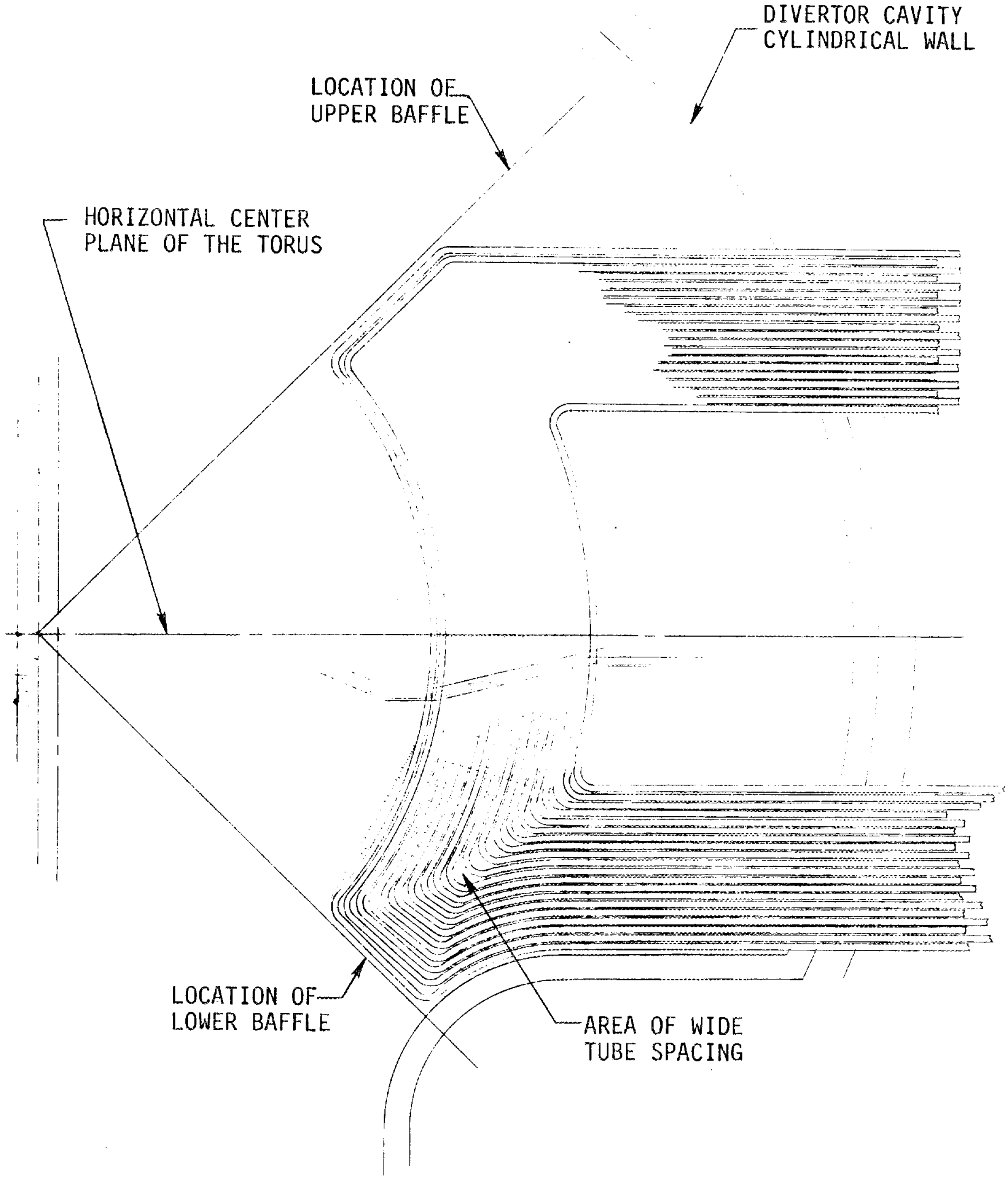

Figure 2-12. Elevation View of the Tube Pattern for the Removable Targets Showing the Wider Tube Spacing at the Corners

- 1×10^{20} ions s^{-1} impinge on the targets; there are two targets

- Essentially all the particles escape from the inner portion of the torus and within a poloidal angle interval of $\pm 30°$ about the equatorial plane; the particle flux distribution is gaussian shaped about the equatorial plane

- The particle flux profile is gaussian-shaped in the radial direction with the total spread being about 9 cm. Actually, two gaussians are assumed in the radial direction with the half-width at half-maximum twice as large outside the separatrix as inside the separatrix

By positioning the targets at an angle of 30° to the incident particles, the particle flux incident on the targets can be reduced by one half.

If the particles were to impact on a bare water-cooled copper target, 8.4×10^{21} atoms/cm^2 would have to be sputtered to remove a 1 mm thickness of surface. The time to erode 1 mm at the location of the peak particle flux would be

$$T_{1mm} = \frac{8.4 \times 10^{21} \text{ atoms cm}^{-2}}{2.5 \times 10^{17} \text{ ions cm}^{-2} \text{ s}^{-1}} \quad \frac{1}{\alpha}$$

or

$$T_{1mm} = 3.4 \times 10^{4} \alpha^{-1} \text{ s}$$

where α = sputtering yield (atoms/ion). Assuming H^+ ions at an energy of $\leq$300 eV, and angle of incidence ~60° from normal,

$\alpha \sim 0.05$[7-8]

and

$T_{1mm} \simeq 6.8 \times 10^5$ s or 190 hours

If an 0.1 mm coating of tungsten were to be plasma-sprayed onto the surface of the copper, the sputtering rate would be greatly reduced (however, there would be enhancement of any x-ray production). The time to erode 0.1 mm of tungsten at the location of the peak particle flux would be

$$T_{0.1\ mm} = 2.4 \times 10^3\ \alpha^{-1}\ s.$$

For H^+ ions at energies of 300 eV $\alpha < 10^{-5}$,[8] and $T_{0.1\ mm} > 2.4 \times 10^8$ s or $> 6 \times 10^4$ hours.

A coating that would be less detrimental (lower Z) to the plasma if any of the sputtered particles should enter the plasma as impurities would be TiC. At the Sandia Laboratories 0.2 mm thick coatings have been plasma sprayed onto copper and under testing exhibited favorable ion erosion characteristics[9]. TiC coating on a graphite subtrate has also been tested as a limiter material in the pulsed tokamak ISX-B[10]. In comparison with other coated limiters and stainless steel limiters it performed well, exhibiting little damage.

For TiC, the time required to erode 0.2 mm at the location of the peak particle flux would be

$$T_{0.2\ mm} = 5.1 \times 10^3\ \alpha^{-1}\ s.$$

This takes into account a porosity of 25% for plasma-sprayed TiC. For ions at an energy of 300 eV and an angle of incidence of 60° to the normal

$$\alpha = 1 \times 10^{-3}\,[9] - 4 \times 10^{-3}\,[8]$$

Therefore, $T_{0.2\ mm} = 5.1 \times 10^6\ s - 1.3 \times 10^6\ s$

or, $T_{0.2\ mm} = 1400\ hr - 360\ hr$

Under the assumptions that have been used, the lifetime of a water-cooled copper target is marginal due to sputtering. A coating of TiC provides a better surface for direct interaction with the plasma; however, if it were to be dispersed throughout the torus its high electrical resistivity may result in some undesirable effects relative to the absorption of microwave power. A coating of tungsten on the copper target would greatly reduce the sputtering, but would constitute a high-Z impurity if any of the sputtered surface would enter the plasma. Tungsten impurities are known to have been the source of severe radiation losses in the PLT device. A tungsten coating has been assumed for the initial targets. However, TiC clad targets could also be tested during the experimental program.

2.6 DIVERTOR CAVITY

This section provides additional information about the divertor cavity which was described briefly in Section 2.2 in conjunction with Figure 2-4. This figure shows the opening in the side walls of the cavity toward the center of the torus where the turbomolecular pumps are attached. The elevation view of the side of the divertor cavity in Figure 2-13 shows that this opening covers approximately 90°. It is made much larger than is required for the pump in order to accommodate the attachment of a large cavity extension box containing ZrAl getter panels or cryopanels which are planned for a divertor upgrade at a later date. The opening, which is covered by a cover plate sealed with an "O" ring, is made as large as possible in order to give the maximum conductance to the pumping panels. The small rectangular notch just below the horizontal center line toward the center of the divertor is provided to clear the electrical bus bar and connector which brings current to the mirror coils. The location of the target chamber baffles at $\pm 45°$ about the horizontal also are shown in Figure 2-13. The lower baffle is very short since it meets the notch in the chamber which provides passage for the pumping ring. The side of the pumping ring notch is in reality part of the lower baffle. The Section A-A inset in Figure 2-13 shows the diagnostic ports which are located at 225°, 270°, and 315° in the in-cavity rim toward the outside of the torus. The

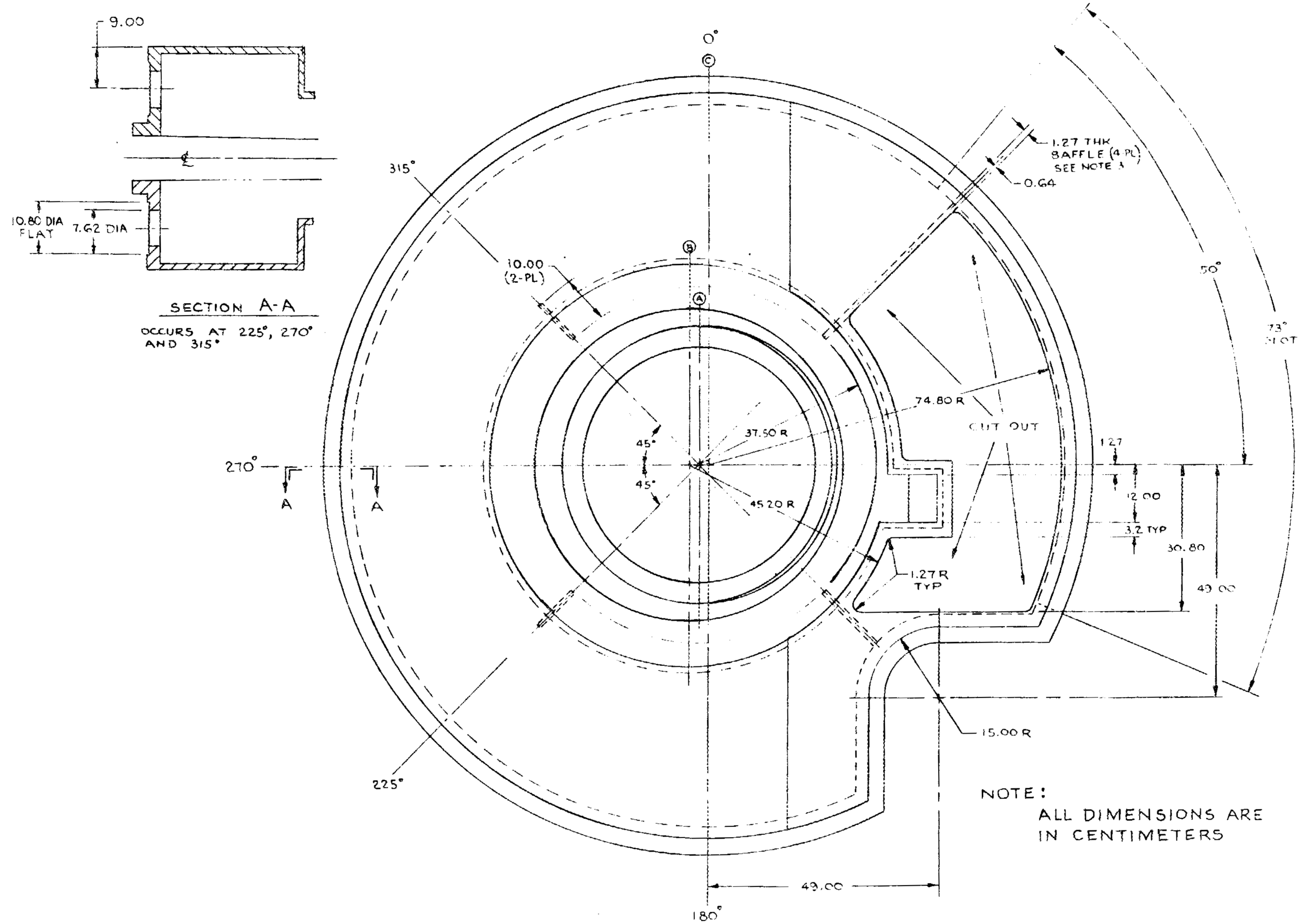

Figure 2-13. Elevation View of the Side of the Divertor Cavity Showing the Notch in the Cover Plate which Provides Clearance for the Mirror Coil Bus Bars

slots for the insertion of the removeable target through the cavity ring toward the inside of the torus are shown in Figure 2-4.

The drawing in Figure 2-14 shows the vacuum cavity dimensioned and independent of the attached components shown in Figure 2-4. This view is useful in understanding the method of manufacture around which the cavity has been designed. The cavity is made of two aluminum weldments which are mirror images of each other. Each weldment is made from a rolled outer flange, a rolled outer cylinder, a machined flat side plate which is bent to form the wedge shaped nose, and a machined hub. The hub is designed so that it can be machined on a lathe face plate by recentering it and tilting the axis as indicated by the letters A, B, C, D, and E in Figure 2-14. The particle channel sidewalls which are obtained by lathe machining are a compromise with the ideal, but as can be seen in Figure 2-4, the contouring to the particle paths is good, especially toward the center of the torus.

2.7 MIRROR COILS

The mirror coils shown in Figure 2-4 are the present mirror coils with new electrical connection tabs and shortened and rebent water leads. There is no machining required on the coil bobbin. Figure 2-4 shows that the original coil tab on the coil side toward the center of the divertor is cut off, but it is not unsoldered from the coil jumper. Resoldering a new lead directly to the coil jumper would probably damage the coil insulation. Extension tabs are brazed to the remaining parts of the original tabs. These extension tabs are bent to go around the compensating coil to the electrical bus connector. This connector has a smaller contact surface than the original connector and it may be necessary to use Multilam® (manufactured by the Multilam Corp., Los Altos, California) washers in its construction in order to keep down the electrical losses. The bus bar from this connector to the neighboring mirror coil must be redesigned.

In their standard configuration, the mirror coil water leads on the side of the mirror coil toward the center of the torus will clearly have an

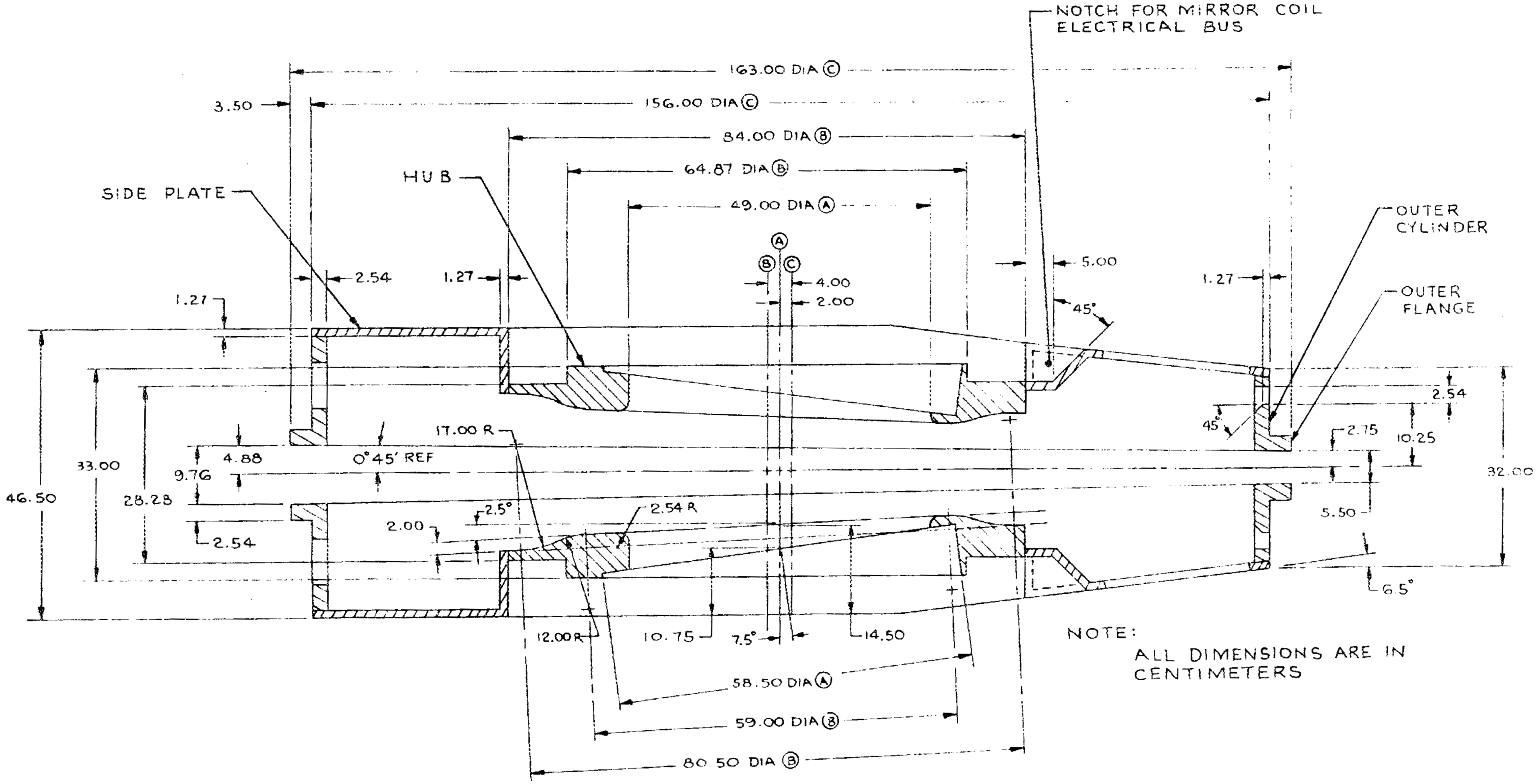

Figure 2-14. Horizontal Plane Cross Section Through the Divertor Cavity Showing the Components of the Weldment Assembly and the Machining-Centers and Axes

interference with the divertor cavity hub and the compensating coil as can be seen in Figure 2-4. Also, it can be seen that there will be no way to get to Swagelok fittings at this location to attach nylon hose. The new design will have insulated copper tube extension to bring the water leads around to the outside of the torus where Swagelok connections can be made to the water hoses. The copper tube extensions which will have a very long life should never need to be replaced as would nylon hose. Replacement of a nylon hose, if they were to be used, would require the removal of the divertor assembly from the torus. The entire divertor is designed so that this should not be necessary for routine maintenance.

The support of the mirror coils is adequately covered in Section 2.2 in the paragraph describing the divertor cavity.

2.8 VACUUM PUMPING OF THE DIVERTOR CHAMBERS

The pumping for the initial installation is to be by the equivalent of two Model TMP 1500 Turbomolecular pumps (manufactured by Leybold-Heraeus, Inc.). These pumps are supported on adaptor tubes which are an integral part of the cover plates over the openings on the cavity side walls, as can be seen in Figure 2-4. They are located on the horizontal center plane and therefore pump on the 90° sectors between the baffles. The adaptors position the pumps so that they do not interfere with either the pumping ring or the diffusion pump valve flange. Figure 2-4 shows that the adaptors contain large viewports which permits a direct view of the particle impingement area on the removable targets.

The divertor cavity is designed to accept, as an upgrade, cavity extensions which may contain either ZrAl getter or cryogenic panel pumps for high pumping speed/low recycle operation of the divertor. These cavity extensions, shown in Figures 2-15 and 2-16, are direct replacements for the cover plates which support the turbopump adaptors in Figures 2-2, 2-3, and 2-4. The pumping of the 90° space between the baffles and the remaining 270° inside the divertor chambers will be independent of each other. In the case of cryopanels, a total of 1.4 m^2 of helium cooled panel would be divided equally between the

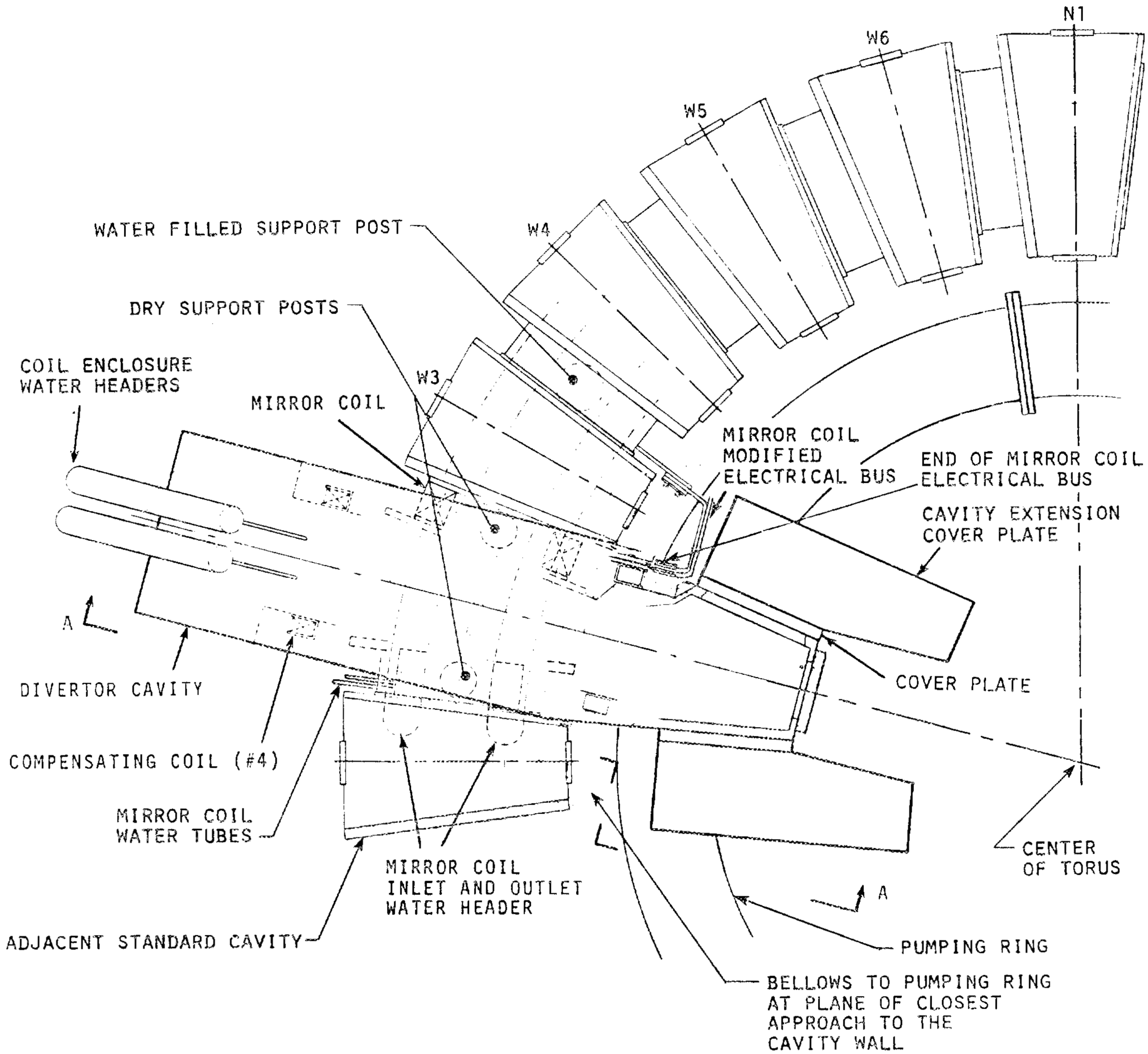

Figure 2-15. Plan View of the Divertor with Pumping Panels Showing Interfaces with the Existing EBT-S

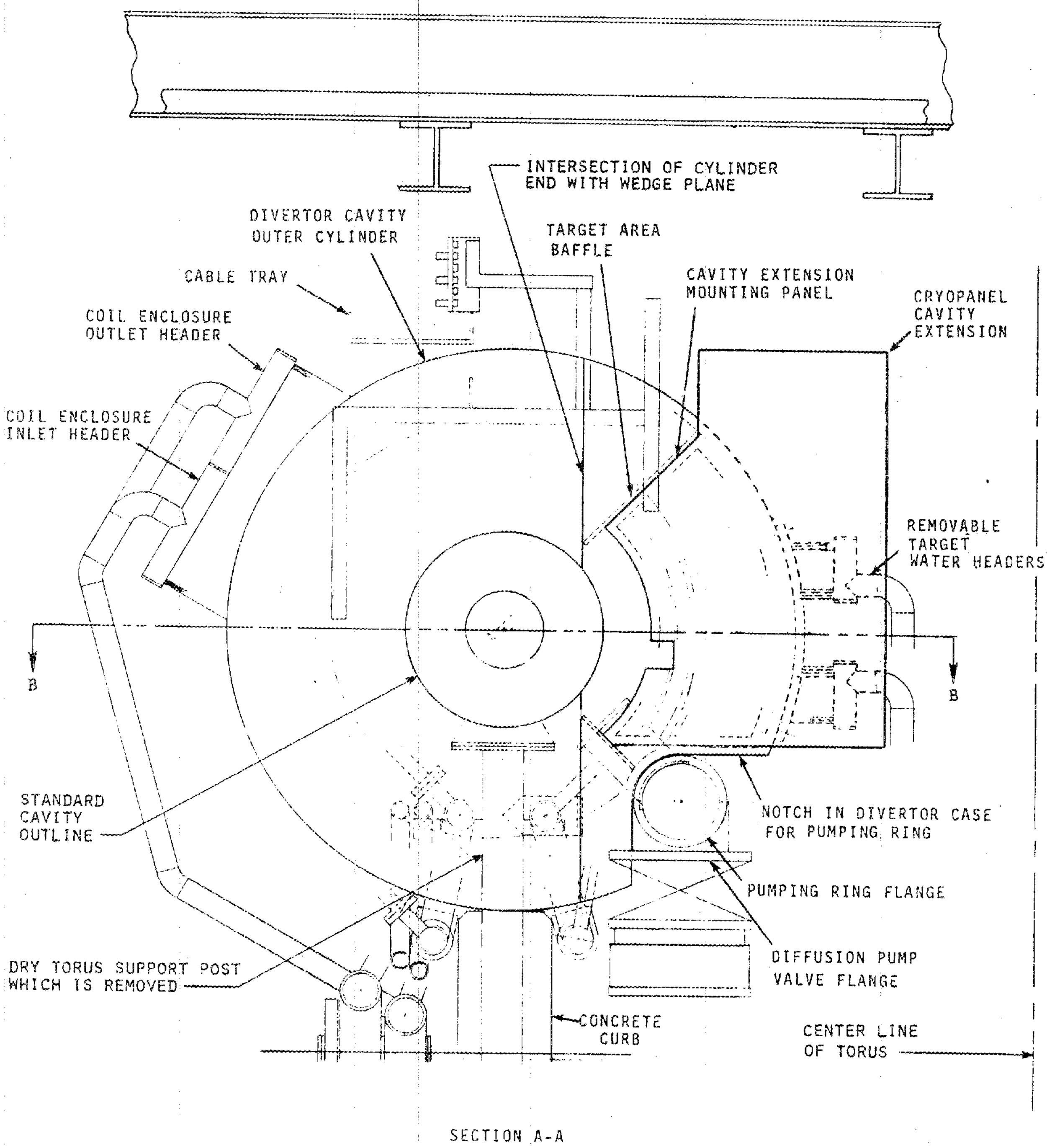

Figure 2-16. Elevation View of the Divertor on Section A-A of Figure 2-2 Showing the Interfaces with the Existing EBT-S

90° and 270° sectors as shown in Figure 2-17. The helium dewar for supplying liquid helium to the cryopanels would be located directly above the divertor on the roof of the EBT-S shielded room. This dewar would be refilled from a transport dewar that is moved into position with the overhead crane.

However, during the initial divertor experiments where the vacuum pumping is provided by the turbo pumps a 30 cm x 30 cm ZrAl getter panel will be tested in a divertor chamber to determine:

- if a microwave shield is required,
- if any baffling is required to prevent atoms sputtered from the target from coating the surface of the bulk getter material,
- if the non-hydrogen pressure levels are sufficiently low that the pumping speed of the ZrAl getter material remains high for a sufficiently long lifetime.

The results of these tests will aid in the selection of a pumping method for the eventual upgrade of the divertor system to allow the high pumping speed/ low recycle mode of operation to be tested. Based on the present geometry for the EBT-S divertor, values for the various pumping speeds, conductances, and pressures associated with operation of the divertor during both high recycling and low recycling of the diverted particles have been calculated. The results were reported in Reference 3. The low pumping speed option will be employed for the initial experimental phase of the divertor experiment. The high pumping speed option will require an upgrade of the system, involving the addition of pumping panels in the divertor cavity and the divertor cavity extension.

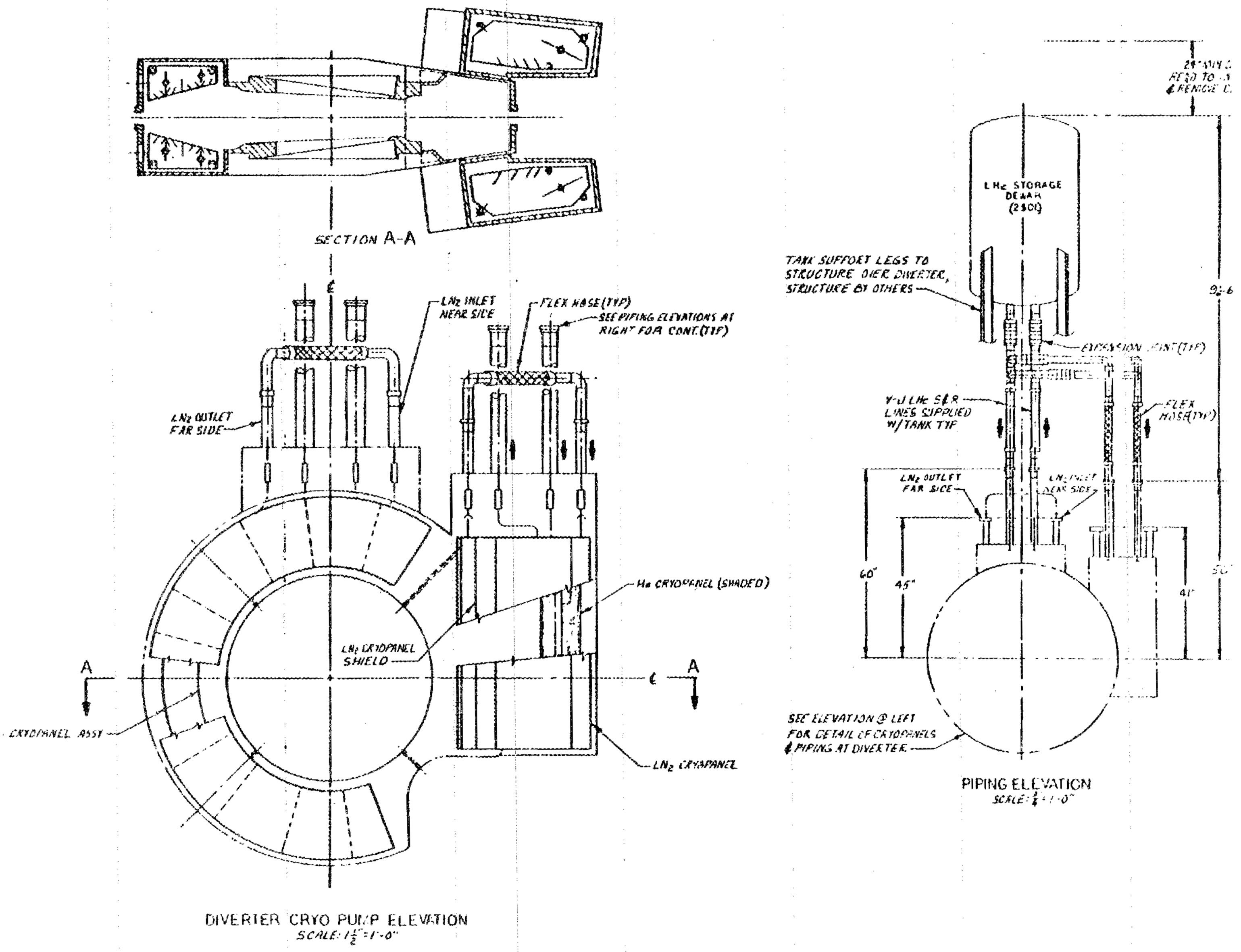

Figure 2-17. Cross Section and Elevation View of the Cryopanels in the 90° and 270° Sectors of the Divertor Cavity

2.8.1 MICROWAVE SHIELDING

No microwave power is introduced directly into the EBT-S cell containing the divertor. However, microwave power can be transmitted into that cell from the adjacent cells. The amount that would be transmitted into the divertor chamber is unknown. In passing through the channels connecting the torus and divertor chamber the microwaves pass through a resonance (2nd harmonic) region that would further attenuate the microwaves. In any event, it may prove necessary to provide microwave shields to prevent arcing in any getter pumps or turbopumps that might be employed, or to prevent heating in cryopanels, etc. However, providing microwave shielding reduces the pumping speed of the vacuum pumping system.

Three sets of square duct dimensions have been calculated that will allow transmission of the 28 GHz microwaves at levels of 10%, 1% or 0.1%. For example, a duct having a cross secion of 0.5 cm x 0.5 cm and a length of 2.4 cm will attenuate the microwaves at 99%. A duct having an area of 0.24 cm x 0.24 cm and a length of 0.39 cm will give the same attentuation. If an array of these ducts, that are spaced by 1 mm to allow for structure, are placed in front of a pumping panel having a pumping speed of 10 ℓ cm^{-2} s^{-1}, the pumping speed would be reduced by 50-60%.

In the pumping analyses referred to in the last section, microwave shields that provide 90% attenuation were considered to be adequate. One such microwave shield was assumed to be placed in each duct connecting the divertor cavity extensions with the main divertor chambers to protect the pumping panels in the cavity extension (or to protect the turbopumps when the extensions are not in place prior to the upgrade). The remaining pumping panels would require a shield located in front of each panel. For 90% attenuation, if as an example, the cross section of the duct is given by 0.5 cm x 0.5 cm, the duct need only be 1 cm in length. This duct will have a higher gas conductance than the ducts which provide a 99% microwave attenuation and there will be a correspondingly smaller effect on the pumping speed of any protected panels. The pumping speed would be reduced by $\sim$40%.

2.9 DIAGNOSTIC INSTRUMENTATION

A cursory study of the diagnostics that might be employed in the divertor chamber has been conducted. The results of this study are presented in this section.

The diagnostic instrumentation for the toroidal divertor has three primary functions, namely:

1) The implementation of automatic go/no-go interlock instrumentation which protects the device and associated power systems from potential damage resulting from abnormal conditions (e.g., loss of coolant etc.);

2) The acquisition of the necessary data which allows the operator and/or automatic feedback systems* to safely control the device and fine tune its operational parameters for optimum performance;

3) The acquisition of data which permits a detailed examination of the diverted ion and electron fluxes and neutral gas densities. This examination will include temporal and spatial measurements of energy spectra and power profiles near the collector surface.

In many instances the same detection instrumentation will serve more than one of the above functions. The third function above is devoted primarily to the evaluaton of divertor performance; however, it has an obvious, though somewhat indirect, influence upon the safe operation and fine tuning process.

---

*It may be desirable to provide automatic tracking of the divertor magnetic field relative to neighboring mirror coil magnetic fields. This tracking could utilize Hall probe sensors and would be designed to maintain the scrape-off flux centered on the target collectors for mirror fields greater than a specified mirror field threshold value. Below this threshold divertor action would be inhibited.

The basic diagnostic instrumentation system that are considered necessary for safe device operation include:

1) Calorimetry - There are four water header paths (see Figure 2-11). Two of these paths are associated with the removable target and two with the remainder of the coil enclosure. It is expected that each of these flow paths will utilize commercially available ΔT and turbine flow transducers to achieve incident power measurements to an accuracy of $\leq 10\%$ (e.g., in a manner similar to that currently used on the PLT neutral beam line calorimeter systems).

2) Thermocouple Arrays - Thermocouples will be distributed to provide the near surface temperature profile associated with the expected power density profile (refer to Figure 2-18 in this report and Figure 6.3 of the Phase I Final Report[3]). A tentative thermocouple location map for the removable target module is shown in Figure 2-19. It is to be noted that an incremental spacing of 1.1 cm is used so that the thermocouples may be located midway between cooling channels as shown in Figure 2-20. It is planned to drill holes from the back side of the copper collector plate to within 0.051 cm of the front surface. The thermocouple junction (diameter = 0.051 cm including sheath) will then be inserted and the copper swaged tightly around the sheath. It is important that each thermocouple be mounted in as nearly the same manner as possible at an equal distance from the surface in good thermal contact with the copper. This manner of mounting should yield good temporal response. This system will require high quality operational amplifiers which will provide a high common mode rejection capability.

   It is expected that identical thermocouple arrays would be utilized on both sides of the inner removable target area and that two identical wider spaced thermocouple arrays would be

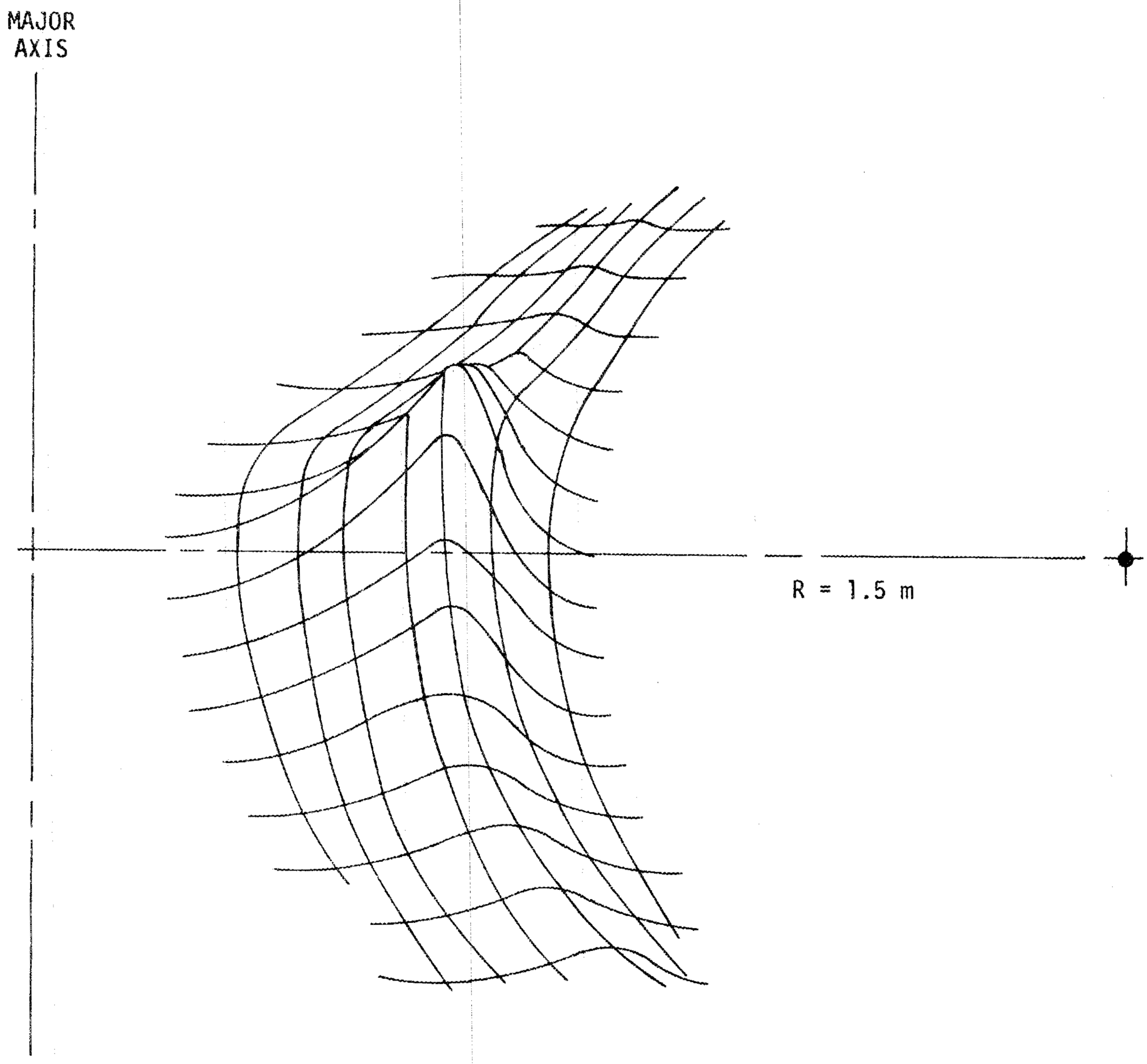

Figure 2-18. Sketch of Expected Power Density Profile (Inner Target Collector)

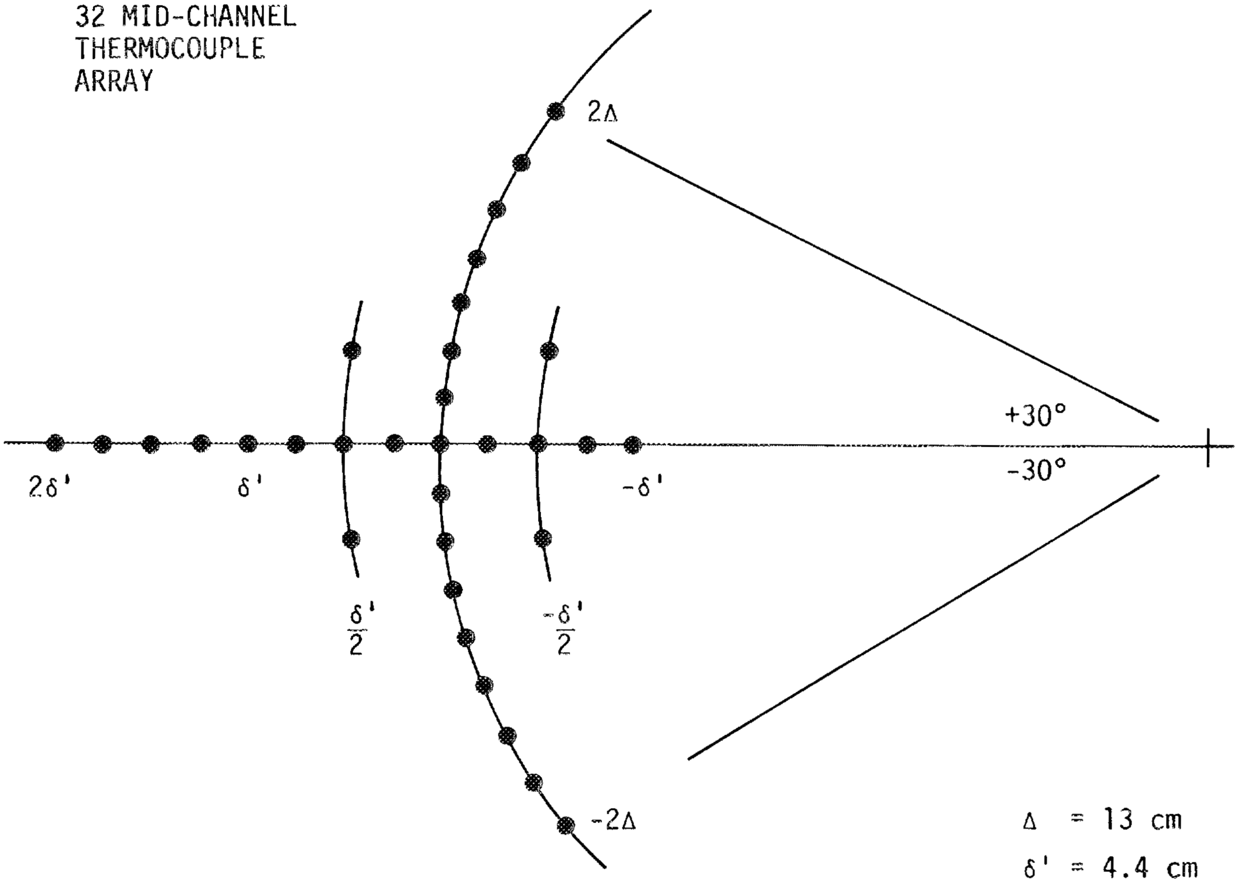

Figure 2-19. Tentative Thermocouple Location Map for Removable Inner Target Collector

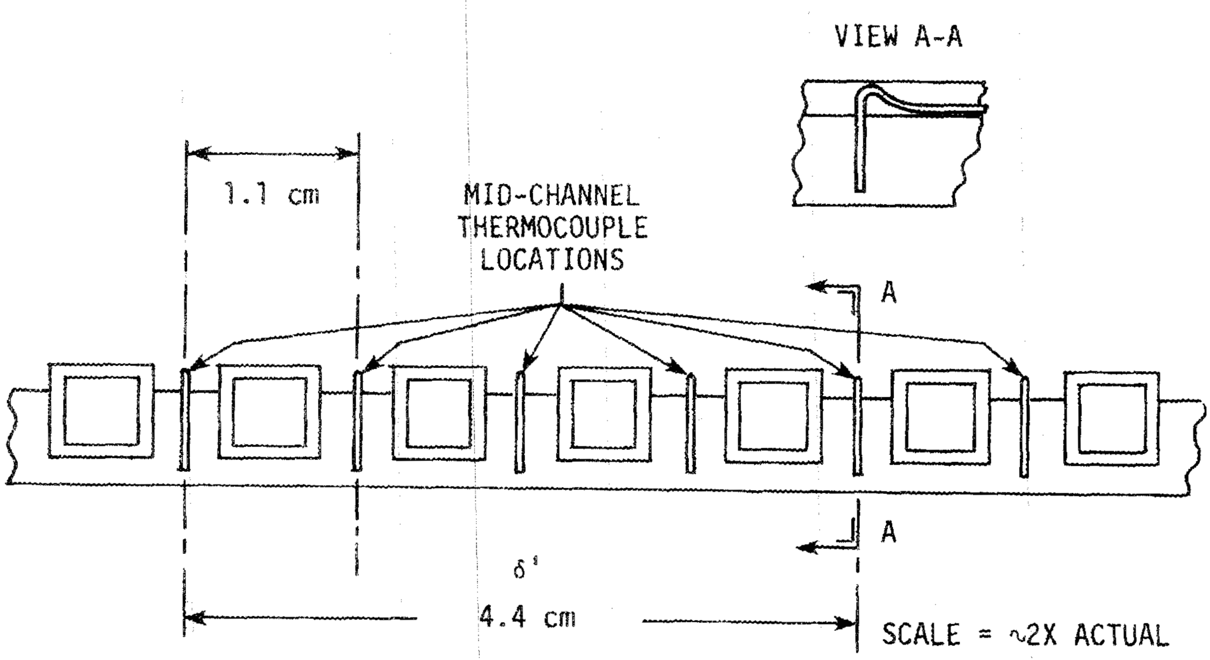

Figure 2-20. Thermocouple Mounting Detail Drawing

utilized on both sides of the outer target area. This will require 128 thermocouple channels in all if 32 channels are required in each case. An additional 32 channels are suggested to be located on the equatorial plane on either side of the divertor entry channels. These locations will be chosen at critical locations for interlock control monitoring of abnormal conditions (e.g., excessive power deposition on the coil end seal, cavity hub areas, etc.).

3) Residual Gas Analyzer and Vacuum Gauges - A residual gas analyzer and vacuum ionization gauges are to be implemented as active monitors of the divertor collector region. The residual gas analyzer will be useful during normal operation (e.g., wall conditioning etc.) and as an early detector for coolant system failure (i.e., water vapor entry). Poor vacuum and/or detection of water vapor may be used to automatically inhibit divertor action, thus protecting the divertor from serious damage.

The above basic diagnostic instrumentation can be expected to satisfy (if interfaced to the appropriate interlock and feedback systems) primary function one and much of what is required for primary function two.

The remaining diagnostic instrumentation can be considered to be dedicated primarily to the quality of divertor performance, rather than operational safety aspects. The following systems would not, for example, be expected to be interfaced with any interlock or automatic control systems. Candidate diagnostic instrumentation which are suggested include the following:

1) Infrared Camera System - This system will provide improved spatial and temporal resolution of surface temperature profiles over that of the thermocouple array. In order for this system to be most effective the camera/s must have a clear view of the divertor collector surface area. Further engineering design is indicated to fully achieve this objective. For example, no provisions have been included for viewing the outer target area.

The inner target IR camera field-of-view is shown on Figures 2-21 and 2-22. As can be seen from Figure 2-22, the field-of-view is most restricted in the vertical (off midplane) direction. This situation can be improved by simply increasing the vertical dimensions of the rectangular section of the turbopump mounting elbow. The use of two color pyrometry techniques is suggested here as a means of obtaining absolute temperature measurements under conditions of decreasing intensity (e.g., sputtered material coating the viewing window). In this technique the ratio of two adjacent wavelengths are used rather than the line intensity. This results in a system which can make temperature measurements which are effectively independent of variations in transmission efficiency.

2) Fluorescence Scrape-Off Layer Diagnostics - Atomic fluorescence spectroscopy offers a sensitive method of measuring very low densities ($\leq 10^6$ atoms cm^{-3}) of metal atoms. Through the use of tunable dye-lasers of suitable intensity, specific fluorescence states can be excited to saturation. Under these conditions the measurement is independent of local density and temperature which are difficult to measure near the divertor collector.

3) X-Ray Diagnostic System/s - Scrape-off layer electrons which would enter the divertor chamber would impinge upon the tungsten or titanium-carbide coated copper targets and generate x-rays. These electrons would come from the bulk toroidal plasma ($T \sim 1$ keV) and the stabilizing electron rings ($T \sim 500$ keV). The resulting x-ray spectra includes two components: (1) a broad continuous spectrum (i.e., due to bremsstrahlung generation) with energy extending to a high energy cutoff equal to the maximum electron energy; and (2) characteristic x-ray line radiation. The characteristic lines for tungsten (viz, $K\alpha = 0.21$ Å or 58 keV and $L\alpha = 1.47$ Å or 8.4 keV) are unique and can be used to identify radiation specific to tungsten. As another example,

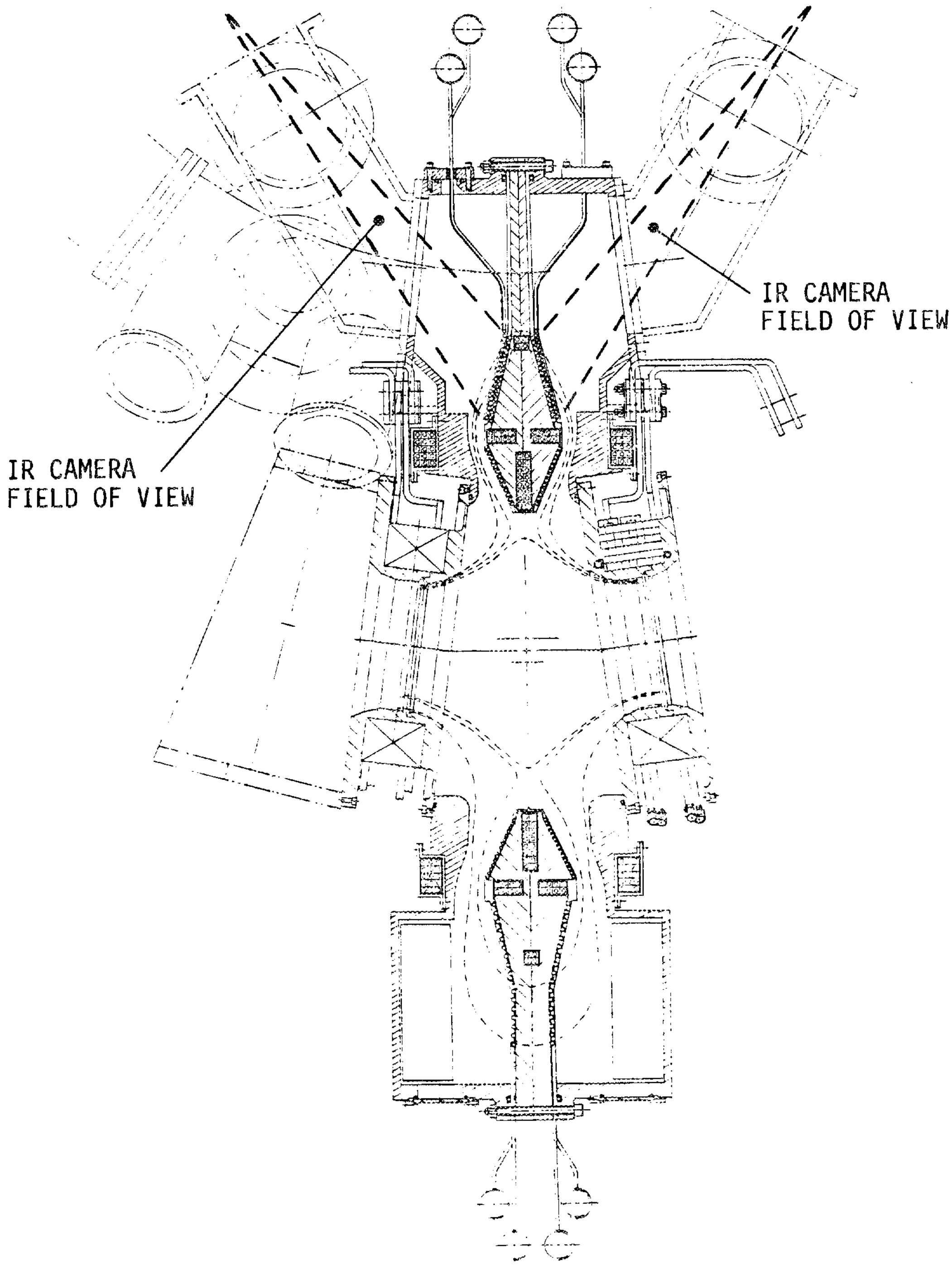

Figure 2-21. Field-of-View for the Infrared Camera Diagnostic; Plan View

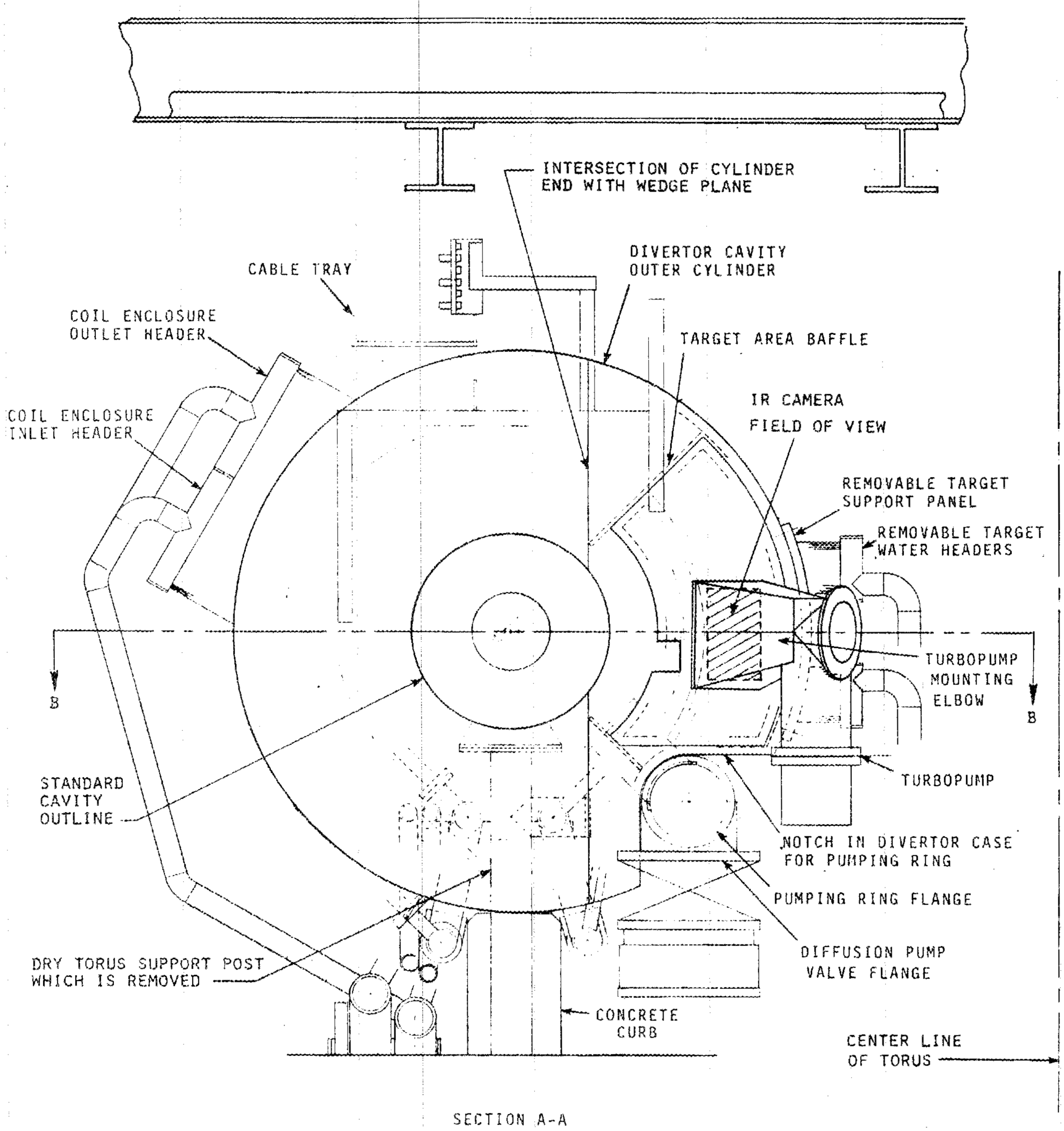

Figure 2-22. Field-of-View for the Infrared Camera Diagnostic; Elevation View

copper has a Kα emission line at 1.54 Å or 8.03 keV). A viable x-ray diagnostic based on the tungsten emission spectra must be adequately shielded and collimated to reduce the background x-ray flux to a tolerable level. This background includes electron ring synchrotron radiation as well as x-ray emission spectra due to electron bombardment of adjacent mirror cavities, throats and other system components. It would appear on the basis of the above considerations, that a useful x-ray diagnostic may be developed utilizing the characteristic line spectra provided the background effects can be suitably reduced. If this is true, either a single movable detector (e.g., a silicon surface barrier) or an array of detectors (well shielded and collimated) would be used to map the tungsten x-ray line spectra (principally the characteristic 58 keV line) to provide the intensity and spatial profiles over the divertor collector surface. The appearance of significant characteristic copper emission lines may be used to monitor the integrity of the tungsten coating. The intensity and spatial information obtained on the tungsten x-radiation may be used to monitor divertor performance.

4) Electric Current Diagnostics - The divertor targets can be electrically insulated so that the resistance to ground can be specified and any net current delivered to them can be measured with standard circuitry. The target may be biased so as to control the escape of secondary emission. This measurement, when correlated with the other diagnostic observations, may represent a simple method of evaluating the performance of the divertor.

3.0 MODIFICATIONS TO THE EBT-S DEVICE AND FACILITY

This section develops the distinction between the divertor assembly, device modifications, and facility modifications. It also describes the status of the engineering on the device and facility modifications at the end of Phase II. The term "device" is used to mean the EBT-S as it presently exists, before the addition of the divertor. The term "facility" is used to mean the building and utilities which are outside the shielded room which houses the EBT-S device. The "divertor assembly" which is described in Section 2.0 includes all of the divertor components which must be added to the EBT-S device. This includes all of the new water headers and electrical buses which one might at first thought consider to be a part of the device modification.

The modifications to the device fall into two groups. The first group includes those modifications which convert an existing device component into a component of the divertor assembly. The second group includes those modifications to the device which are necessary to provide space for the insertion of the divertor assembly.

3.1 DEVICE MODIFICATIONS WHICH ARE PART OF THE DIVERTOR ASSEMBLY

The components which fall into this group are the mirror coils and the mirror coil connecting buses which are adequately described in Section 2.7.

3.2 DEVICE MODIFICATIONS WHICH ARE NOT PART OF THE DIVERTOR ASSEMBLY

The device components in this group are either removed completely or are modified to provide clearance for the insertion of the divertor assembly. There are seven items in this group.

The pumping ring must be modified by the removal of the duct which is located at the divertor. The details of this modification have not been worked out but it is expected that the duct will be sawed off as close to the pumping ring tube outside diameter as possible. The remaining material will be ground off to the outside diameter of the tube and a curved cover plate will be welded over the opening. Figure 2-3 shows that this plate can be on the outer surface of the tube because the size of the notch in the divertor case is fixed by the need to clear the diameter of the pumping ring flange.

The circumferential mirror coil water headers, which are shown with dotted lines behind the divertor cavity in Figure 2-3, must be cut off and an L-shaped extension welded on to bring the water under the divertor cavity. Figure 2-2 shows that these mirror coil inlet and outlet water headers end at the far side of the divertor cavity for cavity locations W2 or N2. The inside header will be brought over the top of the concrete curb because both vertical water risers to the mirror coil hoses will probably be located on the outside of the torus because of an interference with the compensating coils on the inside.

The mirror coil support posts shown in Figures 2-2 and 2-3 will be sawed off flush with the concrete curb. Since these posts are dry in the W2 and N2 locations, no cap is required.

The existing error compensating coils can probably be modified to detour around the outside of the divertor cavity without being rewound. Each of the four coils will be cut at the divertor cavity and a loop added either by splicing turn-by-turn or by using two multipin connectors.

The cable tray will be notched to surround the divertor cavity. The cables in the cable tray will be lifted up so that they will pass over the top of the divertor cavity.

The microwave waveguides above the torus will be rerouted to go over the top of the divertor.

The diagnostics or ion cyclotron heating components, which may be installed on the present EBT-S cavity at the divertor, will be eliminated or moved to other cavity locations.

3.3 FACILITY ADDITIONS

No facility modifications are required but two additions must be made. The divertor coils will be water-cooled. Each coil should have some means of controlling the water flow as the required pressure head varies from coil to coil. The overall water flow will be 6.9 kg/s and the maximum pressure head for any one coil is 446 kPa. The eight inch deionized water line which now brings water to the mirror coils is not large enough to supply the divertor water needs. A new water line to the cooling towers will be required. This facility water line would end just above the floor level where it connects to the divertor water headers.

As described in Section 2.3.5, every effort was made to coordinate the divertor coil current and voltage ratings to make control simple and to minimize the need for additional power supplies. The current ratings were made as nearly equal as possible so that all coils could be connected in series. One overall current regulator will control the coil with the greatest current and electrical shunts across the remaining three coils will bypass locally the current not required by the shunted coil. In the event that the shunt resistances cannot provide fine enough bypass steps a small dc power supply will provide the final adjustment.

It is proposed that one dc generator will supply all the power requirements for the divertor coils. The overall divertor load will be 7893 A with a total series potential of 173 V. One of the available generators at ORNL has a rating of 3 MW at 350 V and consequently has an 8571 A rating.

The second facility addition required is approximately three meters of water cooled electrical bus to bring the divertor current up from an existing bus which ends just under the floor of the EBT-S.

The divertor water lines and the electrical bus can both be brought up through a common hole in the floor just outside the concrete curb at the divertor location as shown in Figure 2-3.

3.4 ADDITIONAL DIVERTOR ASSEMBLY COMPONENTS

The six components in Table 3-1 are considered to be part of the divertor assembly and not device modifications because they do not require any change in the present EBT-S device. They are described in more detail in Sections 2.3.5 and 2.6.

In each case they interface only with the facility additions which are installed just to service the divertor. All of these components, except the divertor coil current modulator, are supported on the divertor vessel with brackets and they could be installed on the divertor assembly prior to its insertion into the torus.

TABLE 3-1

DIVERTOR COMPONENTS WHICH ARE NOT DEVICE MODIFICATIONS

COMPONENT	SHOWN IN FIGURE	DESCRIBED IN PARAGRAPH
COIL ENCLOSURE WATER HEADERS	2-3	2.6
REMOVABLE TARGET WATER HEADERS	2-3	2.6
DIVERTOR COIL WATER HEADERS		2.6
DIVERTOR COIL INTERCONNECTING BUSES		2.3.5
DIVERTOR COIL SUPPLY BUSES		2.3.5
DIVERTOR COIL CURRENT MODULATOR		2.3.5

4.0 CONCLUSION

A toroidal divertor has been engineered in sufficient depth to confirm that a well integrated system can be fabricated and successfully installed into the EBT-S device with a modest and tolerable amount of modification to the EBT-S device and facility. All aspects of the design including mechanical, electrical, structural, thermal, and vacuum aspects have been addressed and a divertor system designed that will meet all the objectives that have been identified. Further engineering of some of the finer details of the design are required before build-to-print drawings are developed, but there are no major design problems still unresolved that would prohibit completion of the design or a successful completion of Phase III of the EBT-S Divertor Program. (Phase III consists of the final design, fabrication and procurement of components, assembly, and installation of the divertor into EBT-S. The Phase III Program Plan and budgetary cost estimate have been provided to ORNL in a separate document.)

5.0 REFERENCES

1. R. A. Dandl, et al., "Research Program for Plasma Confinement and Heating in Elmo Bumpy Torus Devices," Oak Ridge National Laboratory Report, ORNL-TM-4941 (1975).

2. L. A. Berry, C. L. Hedrick, N. A. Uckan, "Elmo Bumpy Torus," Oak Ridge National Laboratory Report, ORNL-TM-6743 (1979).

3. G. Gibson, et al., "A Study of the Feasibility of Installing a Toroidal or Bundle Divertor in EBT-S," Westinghouse Report, WFPS:TME-81-020 (1981).

4. Brechna, H., "Effect of Nuclear Radiation on Organic Materials; Specifically Magnet Insulation in High Energy Accelerators," Technical Report prepared under Contract AT(04-3)-515 for USAEC San Francisco Opertions Office, March 1965.

5. S. K. Borowski, et al, "A Simple Annulus Power Balance in EBT Experiments," Nucl. Fusion 20 (2) (1980) p 177.

6. American Institute of Physics Handbook, First Edition, p. 8-251, McGraw Hill Book Co., Inc., New York, NY (1957).

7. The Plasma/Materials Interaction Task Group OFE, ER, Proceedings of the Workshop on Sputtering Caused by Plasma (Neutral Beam) Surface Interaction, OFE-CONF-790775, Argonne National Laboratory, July 1979.

8. J. Roth, J. Bohdansky, W. Ottenberger, "Data On Low Energy Light Ion Sputtering," Max-Planck-Institut für Plasmaphysik Report, IPP 9/26, May 1979.

9. A. W. Mullendore, et al., "Plasma-Sprayed Coatings for Fusion Reactor Applications," Thin Solid Films 63, pp. 243-249 (1979).

10. R. A. Lengley, et al., "Initial Testing of T_iB_2 and TiC Coated Limiters in ISX-B," J. Nucl. Material 93 and 94, pp. 479-485 (1980).

APPENDIX I

SYSTEMATIC METHOD OF ADJUSTING THE DIVERTOR MAGNETIC FIELD CONFIGURATION

In order for a divertor to be effective, the magnetic field must have a number of properties:

- The null should occur at a prescribed location.

- The separatrix and scrape-off layer guiding the plasma to the target should take a path through a channel which subsequently will hinder back-streaming of neutralized plasma and target debris which would poison the plasma. The magnetic flux should be compressed so that narrow channels can be used; however, there must be adequate clearance on both sides of the separatrix to prevent the diverted plasma from impinging on the channel walls.

- There should be no direct line-of-sight from the divertor target to the plasma.

- The magnetic flux should spread at the location of the target so as to reduce the heat flux being deposited on the target surface via the particles.

It has been found in our studies that in order to satisfy the above constraints the main divertor coil must be divided into three segments, each characterized by a separate number of ampere-turns. Furthermore, to eliminate any tendency of the divertor to alter the net magnetomotive force around the complete torus, compensating coils must be added. For each ampere-turn of the principal coil, a half an ampere-turn (with reverse directional sense) is made to flow in each of two compensating coils.

Because of the number of degrees of freedom, viz, the divertor coil locations and ampere-turns, much time can be consumed in finding a suitable set of parameters. However, a computer code has been developed that is based on a procedure that is described below which allows a systematic design of the divertor coil assembly.

Fine tuning of the divertor is possible to independently adjust the scrape-off layer (via the separatrix origin), adjust or maintain the deposition of plasma on the target, and to control the energy density of particles hitting the target.

Procedure for Magnetic Design of the Divertor

First, establish where the separatrix is to originate, i.e., the location or radius for the magnetic null point. Then perform calculations for the case where the torus is energized normally without divertor currents and determine the following:

BNR the reference flux density at the field null point (located at a preferred radius RN), and

BTR the reference flux density at the preferred target location.

Next, perform calculations assuming only the divertor coils are excited, one subset at a time for coils I, II, and III with compensating currents included, and determine:

BNI the flux density at the null point for one ampere-turn in coil I and minus one-half ampere-turn in each of the compensating coils,

BNII similar information for coil II

BNIII similar information for coil III

BTI the flux density at the target location for one ampere-turn in coil I as outlined above for BNI

BTII similar information for coil II

BTIII similar information for coil III

Equations can now be written in terms of these quantities recognizing that BN = 0 at the null point, and BT = BTREQ, i.e., the desired flux density at the target.

The equations are:

$$BN = BNI\ I_{I} + BNII\ I_{II} + BNIII\ I_{III} + BNR = 0,$$

and

$$BT = BTI\ I_{I} + BTII\ I_{II} + BTIII\ I_{III} + BTR = BTREQ.$$

Assume current I_{III} = A, and solve the equations:

$$BNI\ I_{I} + BNII\ I_{II} = -BNIII\ A - BNR$$

$$BTI\ I_{I} + BTII\ I_{II} = BTREQ - BTIII\ A - BTR$$

Enter the same magnetic field program as was used to determine BTI, BTII, --- BNI --- BTR --- BNR, etc. Include all normal exciting currents and the divertor currents I_{I}, I_{II}, and A.

The output of these calculations should confirm a zero field at the chosen null position and the desired flux density at the chosen target location. Additional output can provide a field map showing the path of the separatrix for the assumed current I_3 = A.

Each time a value of A is chosen, a new separatrix cross-over radius R_{co} will be determined.

Plot as a function of A values of R_{co} and the currents I_I and I_{II}. Draw a curve through the point $R_{co} = f(A)$

Where R_{co} = RT the value of A will be I_{III} for the required solution, and the ordinate through A = I_{III} will give the required value of I_I and I_{II} as well as R_{co} = RT,

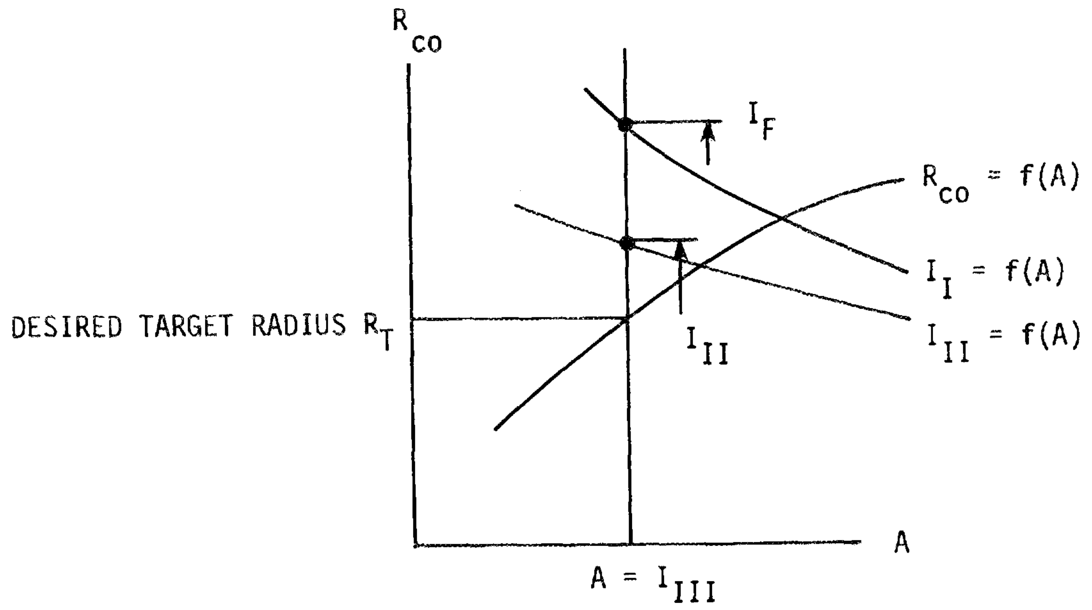

Curve for determining I_{III} for RT and for determining I_I and I_{II} for the desired I_{III}. Curve applies to a particular RN.

For each distinct scrape-off layer origin (the null location RN) the procedure is repeated.

Each time a scrape-off origin is set, plot the value of I_I, I_{II}, and I_{III} as a new curve

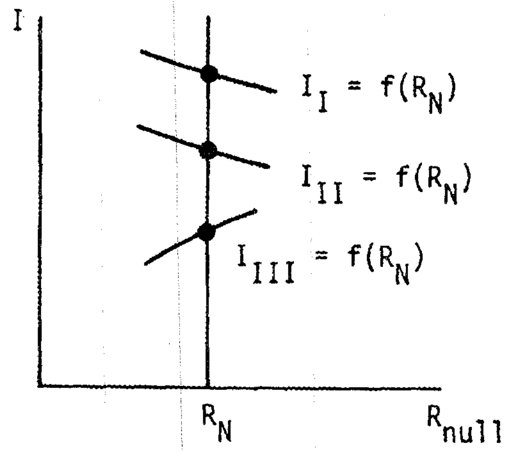

With several values of RN, a satisfactory set of consistent currents can be established for any preferred origin of the separatrix location RN.

EXTERNAL DISTRIBUTION

Director,
Office of Energy Research
U.S. Department of Energy
Mail Stop G-234
Washington, DC 20545

Edwin E. Kintner
Associate Director
Office of Fusion Energy
U.S. Department of Energy
Mail Stop G-234
Washington, DC 20545

Associate Director
Office of Inertial Confinement Fusion
U.S. Department of Energy
Mail Stop G-234
Washington, DC 20545

H. P. Furth
Princeton Plasma Physics Laboratory
Princeton University
P. O. Box 451
Princeton, NJ 08544

Director
Fusion Power Program
Argonne National Laboratory
9700 South Cass Avenue
Argonne, IL 60439

Fusion Power Systems Program Manager
Electric Power Research Institute
P. O. Box 10412
Palo Alto, CA 94303

Director
Fusion Energy Division
Oak Ridge National Laboratory
P. O. Box Y
Oak Ridge, TN 37830

Director
Plasma Fusion Center
Massachusetts Institute of Technology
77 Massachusetts Avenue
Cambridge, MA 02139

Associate Director
Magnetic Fusion Energy
Lawrence Livermore National Laboratory
P. O. Box 808
Livermore, CA 94550

Associate Director for Lasers
Lawrence Livermore National Laboratory
P. O. Box 808
Livermore, CA 94550

CTR Division Leader
Los Alamos National Laboratory
P. O. Box 1663
Los Alamos, NM 87544

ICF Program Manager
Los Alamos National Laboratory
P. O. Box 1663
Los Alamos, NM 87544

Director, Pulsed Energy Programs
Sandia National Laboratory
Albuquerque, NM 87115

R. A. Krakowski
Los Alamos National Laboratory
P. O. Box 1663
Los Alamos, NM 87545

W. B. Ard
McDonnell-Douglas Astronautics Company
St. Louis, MO 63166

J. L. Shohet
Torsatron/Stellarator Program
Electrical and Computer Engr. Dept.
University of Wisconsin
Madison, WI 53706

G. E. Guest
Applied Microwave Plasma Concepts, Inc.
1122 Calle de Los Serranos
San Marcos, CA 92069

R. A. Dandl
Applied Microwave Plasma Concepts, Inc.
1122 Calle de Los Serranos
San Marcos, CA 92069

Dr. George Miley
Department of Nuclear and
Electrical Engineering
University of Illinois
214 Nuclear Engineering Laboratory
Urbana, IL 61801

P. M. Meade
J. C. Sinnis
J. A. Schmidt
G. Sheffield
J. Johnson
D. Grove
Princeton University
Plasma Physics Laboratory
P. O. Box 451
Princeton, NJ 08544

B. Montgomery
T. F. Yang
E. Rappaport
Plasma Fusion Center
Massachusetts Institute of Technology
Cambridge, MA 02139

J. Clarke
Dr. Anne N. Davies
J. F. Decker
W. F. Dove
R. J. Dowling
W. R. Ellis
G. Haas
D. Nelson
J. M. Turner
Department of Energy
Mail Stop G-234
Washington, DC 20545

L. A. Berry
R. Colchin
R. A. Dory
G. R. Haste
C. L. Hedrick
M. S. Lubell
L. Owen
J. Sheffield
D. Steiner
T. Tucker
Oak Ridge National Laboratory
P. O. Box Y
Oak Ridge, TN 37830

FUSION POWER SYSTEMS
PITTSBURGH, PENNSYLVANIA

INTERNAL DOCUMENT DISTRIBUTION SHEET

EFERENCE NO: WFPS:TME-81-026
ATE: September 29, 1981
ONTRACT: Sub 22X-21086C
ROJECT/WBS CATEGORY:

AUTHOR(s): G. Gibson, et al.
TITLE: EBT-S DIVERTOR PROJECT - PHASE II - FINAL REPORT ENGINEERING DESIGN OF A TOROIDAL DIVERTOR FOR THE EBT-S FUSION DEVICE

PPROVAL/RELEASE CATEGORY

- [ ] DRAFT FOR REVIEW AND COMMENT
- [ ] DRAFT FOR INFORMATION ONLY
- [ ] PRELIMINARY RELEASE - INTERNAL PROJECT USE
- [x] APPROVED BY W FOR RELEASE - SUBJECT TO APPROVAL OF: ORNL/DOE

C	A	NAME
X		SHAPIRO, Z. M.
X		KLEIN, D.
X		ROSE, R. P.
X		VARLJEN, T. C.
X		FLANAGAN, C. A.
X		HALEY, T. E.
X		GIBSON, G.
X		HECK, F. M.
X		MALICK, F. S.
X		SUCOV, E. W.
X		BRENNER, W. C.
		CHAPIN, D. L.
		CHI, J. W. H.
X		CHIANESE, R. B.
		CROTZER, M.E.
X		EASOZ, J. R.
		GARBER, H. J.
X		GOLD, R. E.
		GREEN, L.
		IBRAHIM, E. A.
X		IWINSKI, E. M.
		JEDRUCH, J.

C	A	NAME
X		KARBOWSKI, J. S.
		KYSLINGER, J. A.
X		LEE, A. Y.
X		MAI, L. P.
		MILLER, J. W.
		ROGOSKY, D.
X		RUCK, G. W.
X		SINK, D. A.
		SNIDERMAN, M.
X		STOOKSBERRY, R. W.
X		FPS ENGINEERING OFFICE (1)

C	A	NAME
		JONES, A. R. (AESD)
		WRIGHT, M. K. (AESD)
		CREAGAN, R. J. (R&D)
		KILGORE, L. A. (E.PGH)
		WHITNEY, E. C. (E.PGH)
		FINK, J. H.
X		KOVACIK, W. P. (R&D)
		HAUN, R. D. (R&D)
X		JONES, C. K. (R&D)
		OLSEN, R. D. (R&D)
		PARKER, J. H. (R&D)
		THOMPSON, F. T. (R&D)
		WARREN, R. W. (WLASL)
		LIBERMAN, I. (WLASL)
		GROVE, D. J. (WPPPL)
		JOHNSON, J. L. (WPPPL)
X		YOUNG, J. L. (R&D)
		RIEDEL, E. P. (R&D)
		HOLLAND, J. R. (R&D)
X		Nahemow, M. (R&D)
X		AESD Library
X		ARD Library
X		NES Library
X		R&D Library

COMMENTS

APPROVED BY: TW

A- ABSTRACT ONLY
C - COMPLETE COPY

REFERENCE NO: WFPS:TME-81-026
TITLE: PHASE II - FINAL REPORT EBT-S DIVERTOR PROJECT
AUTHOR: G. GIBSON, et al.